The synaptic vesicle SNARE neuronal Synaptobrevin promotes endolysosomal degradation and prevents neurodegeneration

Adam Haberman,[1] W. Ryan Williamson,[1] Daniel Epstein,[1] Dong Wang,[1] Srisha Rina,[1] Ian A. Meinertzhagen,[3,4] and P. Robin Hiesinger[1,2]

[1]Department of Physiology and [2]Green Center for Systems Biology, University of Texas Southwestern Medical Center, Dallas, TX 75390
[3]Neuroscience Institute; and [4]Department of Psychology, Life Science Centre; Dalhousie University, Halifax, Nova Scotia B3H 4J1, Canada

Soluble NSF attachment protein receptors (SNAREs) are the core proteins in membrane fusion. The neuron-specific synaptic v-SNARE *n-syb* (*neuronal Synaptobrevin*) plays a key role during synaptic vesicle exocytosis. In this paper, we report that loss of *n-syb* caused slow neurodegeneration independent of its role in neurotransmitter release in adult *Drosophila melanogaster* photoreceptor neurons. In addition to synaptic vesicles, n-Syb localized to endosomal vesicles. Loss of *n-syb* lead to endosomal accumulations, transmembrane protein degradation defects, and a secondary increase in autophagy. Our evidence suggests a primary defect of impaired delivery of vesicles that contain degradation proteins, including the acidification-activated Cathepsin proteases and the neuron-specific proton pump and V0 adenosine triphosphatase component V100. Overexpressing V100 partially rescued *n-syb*–dependent degeneration through an acidification-independent endosomal sorting mechanism. Collectively, these findings reveal a role for n-Syb in a neuron-specific sort-and-degrade mechanism that protects neurons from degeneration. Our findings further shed light on which intraneuronal compartments exhibit increased or decreased neurotoxicity.

Introduction

Regulated SNARE-mediated membrane fusion underlies a plethora of intracellular trafficking, sorting, and exocytosis and has been particularly well studied in neurotransmitter release (Südhof and Rothman, 2009). The synaptic v-SNARE n-Syb (neuronal Synaptobrevin)/VAMP2 is a key protein required for synaptic vesicle exocytosis (Sweeney et al., 1995; Deitcher et al., 1998; Schoch et al., 2001). In *Drosophila melanogaster*, n-Syb is a neuronal protein that functions partially redundantly with the ubiquitously expressed Cellubrevin (Bhattacharya et al., 2002). Thus, n-Syb represents one of several intracellular membrane trafficking proteins that serve specialized neuronal requirements for vesicle trafficking at the synapse.

In addition to the synaptic vesicle cycle, neurons use specialized membrane trafficking (Chan et al., 2011) and a neuronal intracellular degradation mechanism during development and adult maintenance (Williamson et al., 2010a,b). Loss of endolysosomal or autophagosomal degradation is sufficient to cause adult-onset degeneration in *Drosophila* photoreceptors (Lee and Montell, 2004; Xu et al., 2004; Akbar et al., 2009; Williamson et al., 2010a) and neurons in general (Hara et al., 2006; Komatsu et al., 2006; Nixon et al., 2008). Autophagy and the canonical endolysosomal system are considered ubiquitous cellular membrane trafficking machinery that may serve specialized or increased functions in neurons. In addition to the ubiquitous degradation machinery, we recently reported that a neuronal vesicle ATPase (v-ATPase) component provides a neuron-specific intracellular degradation mechanism; loss of *v100*, the neuron-specific v-ATPase subunit a1, leads to defects in brain

Correspondence to P. Robin Hiesinger: robin.hiesinger@utsouthwestern.edu

A. Haberman's present address is Oberlin College, Oberlin, OH 44074.

S. Rina's present address is Dept. of Molecular Genetics, University of Texas Southwestern Medical Center, Dallas, TX 75390.

Abbreviations used in this paper: AVD, degradative autophagosomal vacuole; AVI, immature autophagosomal vacuole; ERG, electroretinogram; TNT, tetanus toxin light chain; UAS, upstream activation sequence; v-ATPase, vesicle ATPase.

© 2012 Haberman et al. This article is distributed under the terms of an Attribution–Noncommercial–Share Alike–No Mirror Sites license for the first six months after the publication date (see http://www.rupress.org/terms). After six months it is available under a Creative Commons License (Attribution–Noncommercial–Share Alike 3.0 Unported license, as described at http://creativecommons.org/licenses/by-nc-sa/3.0/).

The Rockefeller University Press $30.00
J. Cell Biol. Vol. 196 No. 2 261–276
www.jcb.org/cgi/doi/10.1083/jcb.201108088

wiring (Williamson et al., 2010b) and adult-onset degeneration (Williamson et al., 2010a) in *Drosophila.* To our knowledge, no other neuron-specific membrane trafficking protein required for intracellular degradation has so far been characterized.

We have previously reported that loss of *n-syb* in the *Drosophila* visual system leads to fine structural synaptic defects that have an onset before synapse formation (Hiesinger et al., 1999). Recent work has shown that *v100* behaves similarly to *n-syb*. Specifically, loss of either protein leads to neurotransmitter release defects, and both proteins directly interact with the t-SNAREs Syntaxin and SNAP-25 at the synapse (Hiesinger et al., 2005). These observations give rise to the idea that both proteins might exert related functions in endolysosomal trafficking in addition to their roles in neurotransmitter release. Here, we show that loss of *n-syb* causes intracellular degradation defects that lead to neurodegeneration in adult photoreceptor neurons. n-Syb functions in concert with V100 in a neuronal sort-and-degrade mechanism that is required for neuronal maintenance independent of their roles in neurotransmitter release.

Results

Loss of *n-syb* causes slow degeneration in adult photoreceptor neurons

We previously reported remarkable similarities between the v-SNARE n-Syb and the v-ATPase component V100 during synaptic development (Hiesinger et al., 1999; Williamson et al., 2010b) and in synaptic function (Hiesinger et al., 2005). In addition, we have shown that *v100* is required to maintain neurons and that this role is independent of its function on synaptic vesicles (Williamson et al., 2010a). To investigate a possible similar function of n-Syb in maintaining neurons, we investigated the morphology and function of *n-syb* mutant photoreceptor neurons over time compared with photoreceptors mutant for *v100.* We used the *ey3.5FLP* method to selectively generate *n-syb* mutant photoreceptors in otherwise heterozygous animals (Chotard et al., 2005; Mehta et al., 2005). To assay degeneration morphologically, we assessed the loss of rhabdomeres, actin-rich extensions of the photoreceptor apical membrane that contain the light-sensitive Rhodopsin (Harris et al., 1976). To assay degeneration functionally, we recorded electroretinograms (ERGs), extracellular recordings that measure the response of photoreceptors to a light stimulus (Heisenberg, 1971). As shown in Fig. 1, adult *n-syb* mutant photoreceptors exhibited slow neurodegeneration as indicated by a significant loss in the number of intact rhabdomeres and ERG depolarization in 1- and 5-wk-old flies compared with controls (Fig. 1, A, C, F, and H). The progressive reduction in the ERG response amplitude is accelerated by exposure to constant light and rescued by photoreceptor-specific expression of wild-type *n-syb* (Fig. 1, D and I). The degeneration phenotype is similar to, but milder than, the phenotype observed for *v100* (Fig. 1, B and G). We further compared loss of *n-syb* or *v100* to loss of *syt* (*synaptotagmin*), which plays critical roles in both synaptic vesicle exocytosis and endocytosis in *Drosophila* photoreceptors (Littleton et al., 1993; Reist et al., 1998). In contrast to *n-syb* and *v100*, photoreceptors lacking *syt* exhibited no signs of functional or morphological degeneration, indicating that defective synaptic vesicle cycling does not reduce photoreceptor viability (Fig. 1, E and J–L). Similarly, loss of neurotransmission in a mutant for histamine (hdc^{jk910}; Burg et al., 1993), the neurotransmitter of *Drosophila* photoreceptors, caused neither structural nor functional degeneration (Fig. S1). Collectively, our findings reveal that loss of *n-syb* results in slow degeneration in a manner similar to *v100*. Comparison with *syt* and a mutant lacking a neurotransmitter further suggests that degeneration is caused by a mechanism that is independent of neurotransmitter release.

n-Syb localizes to synaptic endosomal compartments as well as synaptic vesicles

If Syb has a role in maintaining neurons independent of its function in neurotransmitter release, this role is likely to be independent of synaptic vesicles. At synapses, n-Syb colocalized with all synaptic vesicle markers, including Syt and V100 (Fig. 2, A–C). In addition, n-Syb colocalized to a large extent with the early endosomal markers Syx7 (Syntaxin 7)/Avalanche and Rab5 but less extensively with markers of two different endosome types, Hrs and the recycling endosomal marker Rab11, or with several late endosomal and lysosomal markers (Fig. 2 B). We further verified the immunohistochemical colocalization results using YFP-tagged overexpression constructs for Rab5, Rab7, and Rab11. n-Syb colocalized at synapses most extensively with the early endosomal marker Rab5, significantly less with the late endosomal marker Rab7, and only little with the recycling endosomal marker Rab11 (Fig. 2, D–F; quantification is shown in Fig. 2 B, green bars). The colocalization with Rab5 was most prominent at the synaptic terminals (Fig. 2 D, arrow), whereas in the cell bodies, n-Syb colocalized only partly with the endolysosomal markers analyzed here (Fig. 2 D, arrowhead). We corroborated these findings using high-resolution 3D deconvolution that allows to discern individual compartments at the resolution limit of light (Hiesinger et al., 2001). In the synaptic regions of the optic lobe, n-Syb largely colocalized with Syx7- and V100-positive compartments (Fig. 2 G, arrow). In cell bodies, clearly discernible endosomal compartments are visible after deconvolution, which are positive for different combinations of n-Syb, Syx7, V100, and Rab5 (Fig. 2, G [arrowhead] and H). These findings indicate that in addition to synaptic vesicles, n-Syb localizes to a subset of early endosomal compartments, predominantly at synapses.

Loss of n-Syb results in accumulations of several types of undegraded intracellular membrane compartments

We have previously reported that loss of functional n-Syb leads to intracellular accumulations of transmembrane receptors and late developmental defects in the optic lobe (Hiesinger et al., 1999). In early experiments, we used tetanus toxin light chain (TNT) expression, which specifically cleaves n-Syb but not n-Syb's closest homologue Cellubrevin (Sweeney et al., 1995). Photoreceptor-specific expression of TNT mimics all *n-syb* loss-of-function phenotypes, including impaired synaptic development (Hiesinger et al., 1999) and neurotransmitter release (Sweeney et al., 1995), as well as degeneration of photoreceptors

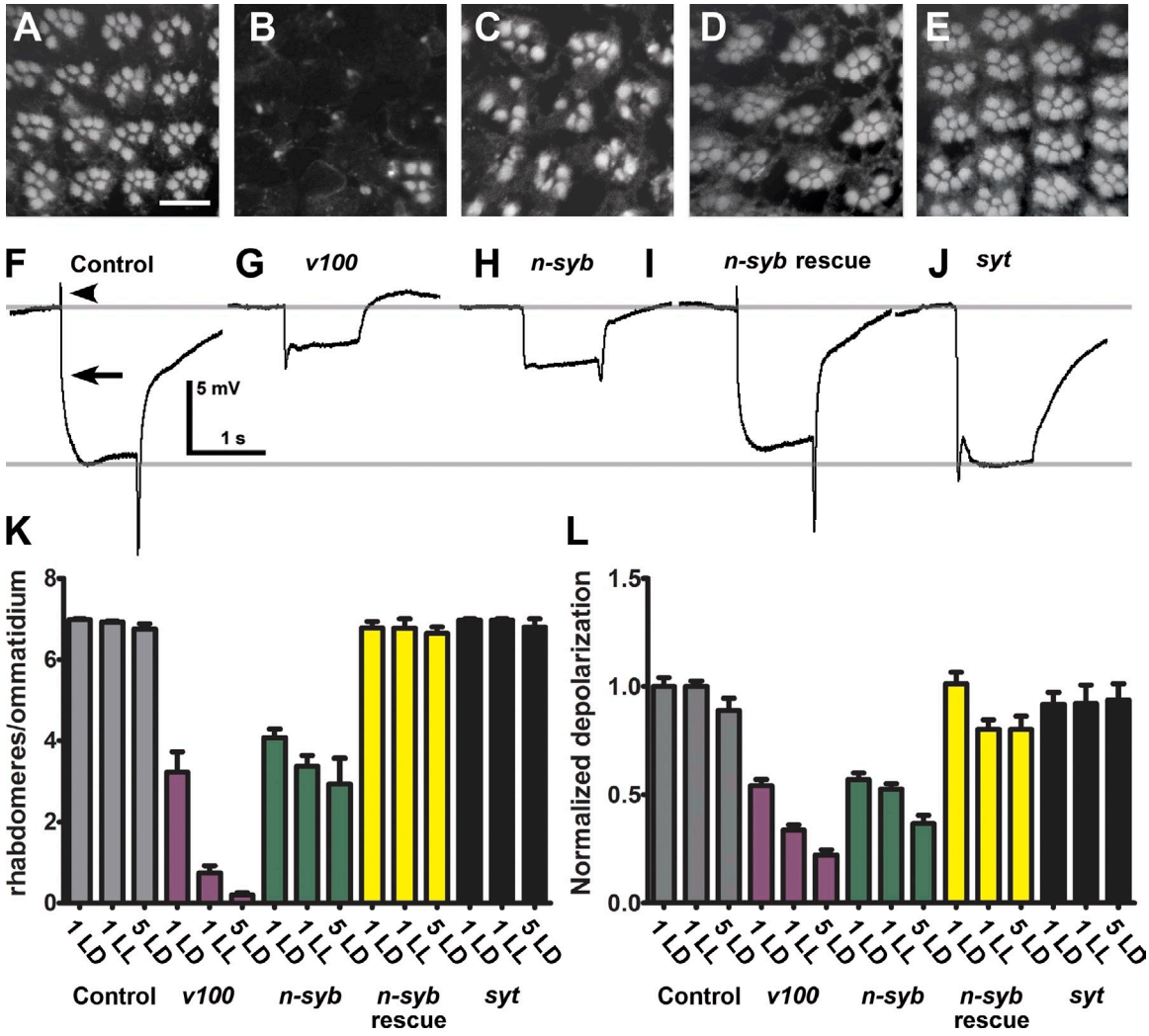

Figure 1. **Loss of *n-syb* causes slow degeneration in adult photoreceptor neurons.** (A–E) Phalloidin labeling of rhabdomere profiles from ommatidial cross sections of 5-wk-old adult *Drosophila* eyes provides a morphological index of photoreceptor degeneration. Compared with wild type (A), rhabdomeres are mostly lost in *v100* (B), partially lost in *n-syb* (C), rescued in the *n-syb* mutant by photoreceptor-specific *n-syb* expression (D), and normal in *syt* (E). (F–J) ERG recordings provide a functional measure of photoreceptor integrity. ERG recordings are shown from 5-wk-old wild-type (F), *v100* (G), *n-syb* (H), *n-syb* rescue (I), and *syt* (J) eyes. Note normal size of sustained negative photoreceptor response (arrow in F) in F, I, and J and reduced on transients (arrowhead in F) in G, H, and J, indicating loss of neurotransmission. (K) Counts of rhabdomeres/ommatidium for 1-wk-old flies raised in 12-h light/dark cycles (1LD), constant light (1LL), and 5 wk of light/dark cycles (5LD). (L) Magnitude of ERG depolarization normalized to wild-type photoreceptor response (arrow in F). Bar, 10 µm. All error bars are SEM for $n > 50$ for all experiments.

(unpublished data). To assess the intracellular trafficking defects potentially underlying these developmental and degenerative phenotypes, we undertook transmission EM of the synaptic terminals in the first optic neuropil, or lamina. As shown in Fig. 3, both TNT expression and loss of *n-syb* caused indistinguishable defects. Most prominently, the terminals are filled with vesicles, which we have previously observed and interpreted as synaptic vesicle accumulations caused by a defect in exocytosis (Hiesinger et al., 2005). In addition, both TNT expression and loss of *n-syb* caused a disorganization of photoreceptor terminals in the synaptic cartridges of the lamina and have widely varying profile sizes in cross sections, whereas their active zone numbers are unaltered (Fig. S2 and Fig. 3, F and G). In contrast, *syt* mutant terminals appeared devoid of vesicles and exhibited no increase in their size (Fig. 3, E and F), consistent with previous observations (Reist et al., 1998). These data show that loss of *n-syb*, but not *syt*, causes a pronounced increase in vesicle content and a several-fold increase in the profile size of synaptic terminals.

Next, we assessed the appearance of late degradative compartments, i.e., multilamellar lysosomal structures (Dermaut et al., 2005) and autophagosomal compartments as recognized by double membranes (Williamson et al., 2010a). For both TNT expression and *n-syb*–deficient photoreceptor terminals, we found no increase in the appearance of multilamellar lysosomal structures, which occur when degradation in lysosomes is defective (Dermaut et al., 2005; Schultz et al., 2011). However, we did find multivesicular and autophagosomal compartments that are not observed in wild type or *syt* (Fig. 3, B and D, arrows). These phenotypes were also similar to *v100* (Williamson et al., 2010a). We further assessed the emergence of these ultrastructural defects after photoreceptor-specific TNT expression,

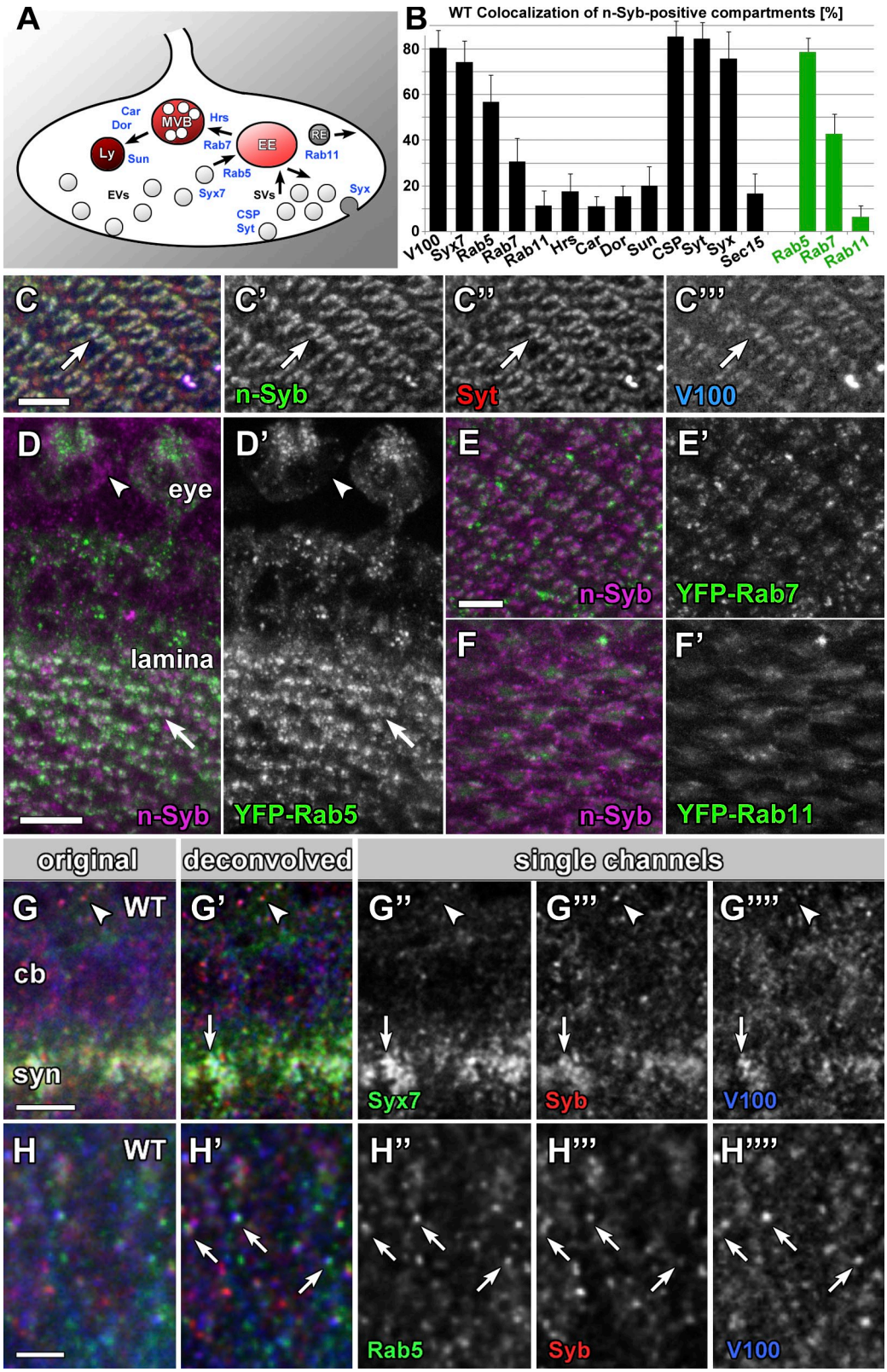

Figure 2. **n-Syb localizes to synaptic endosomal compartments in addition to synaptic vesicles.** (A) Intracellular compartments in a wild-type synaptic terminal. Cysteine string protein (CSP), Synaptotagmin (Syt), and the t-SNARE Syntaxin 1A (Syx) function in synaptic vesicle (SV) exocytosis. Early endosomes (EE) and endosomal vesicles (EV) are marked by Rab5 and Avalanche/Syntaxin 7 (Syx7). Early endosomes undergo degradation via multivesicular body (MVB) formation, marked by Rab7 and Hrs, and lysosomes (Ly) marked by carnation (Car), deep orange (Dor), and sunglasses (Sun). Recycling endosomes (RE) are marked by Rab11. (B) Colocalization of 16 markers with n-Syb in developing photoreceptor terminals at ~P+30%. Shown are the percentiles of individually distinguishable compartments for immunolabeling with 13 antibodies (black bars) that are positive for n-Syb coimmunolabeling. Green bars show similar quantification of n-Syb colocalization for compartments marked by YFP-tagged Rab5, Rab7, and Rab11. (C–H'''') Immunolabeling of photoreceptor terminals at ~P+30%. (C) Immunolabeling for n-Syb, Syx7, and Hrs (green). Single channels are shown in C'–C'''. (D–F) Colabeling of *n-syb*-Gal4>YFP-Rab5 (D),

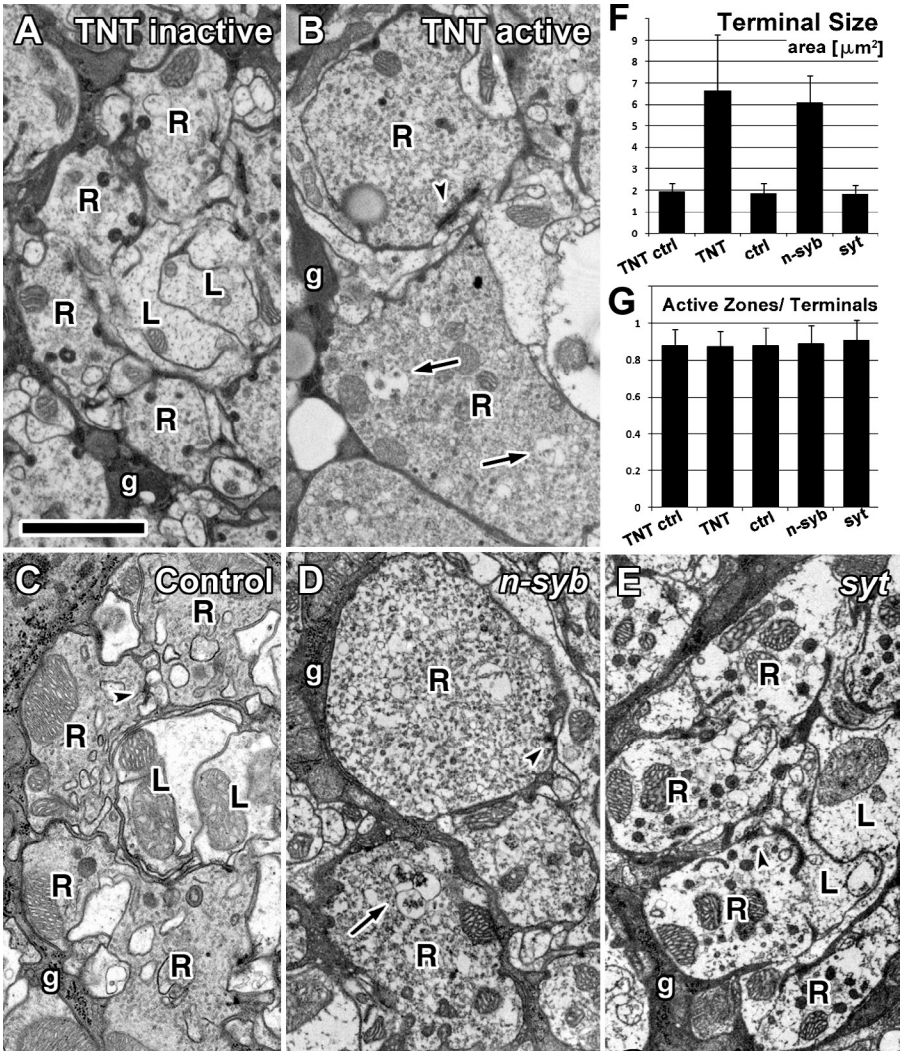

Figure 3. **Loss of *n-syb* causes accumulations of several types of undegraded intracellular membrane compartments.** (A–E) Electron micrographs of photoreceptor terminals in the lamina for photoreceptor-specific expression of inactive TNT (A), active TNT (B), wild-type control (ctrl; C), *n-syb* mutant photoreceptor terminals (D), and *syt* mutant photoreceptors (E). R, photoreceptor terminal profiles; L, postsynaptic lamina cells; g, glia; arrows show autophagosomal compartments, and arrowheads display tetrad synapses. (F) Terminal size shown from mean profile areas for TNT, control *n-syb*, and *n-syt* terminals. Only *TNT active* and *n-syb* are significantly different compared with controls and *syt* ($P < 0.01$). Note that both TNT and *n-syb* also show very high variability of terminal sizes, as indicated by the large SEM. (G) Counts of tetrad active zone profiles per photoreceptor terminal profile. All error bars are SEM. Bar, 1 µm.

from EM observations of terminals at 50 and 75% of pupal development (P+50% and P+75%). An increased overall vesicle density caused the appearance of darkened photoreceptor terminals as early as P+50% (Fig. S3). In addition, terminals at P+75% exhibited numerous larger vesicular structures that have the appearance of multivesicular bodies but lack an obvious double-membrane envelope. Together, these data indicate that intracellular vesicle accumulations at *n-syb* mutant terminals start during development, with an increase of small vesicle density before the emergence of multivesicular bodies before eclosion and autophagosomes in the adult.

Loss of *n-syb* results in accumulations of endosomal vesicles

To assess the molecular nature of the intracellular accumulations observed with EM, we performed wild-type colocalization analyses. To assess even subtle level changes between mutant and wild-type terminals precisely, we generated 50% mutant *n-syb* mosaics (Fig. 4 A). The early endosome marker Syx7 in particular revealed a striking image of the photoreceptor terminal field with many substantially enlarged terminals and little to no recognizable cartridge structure (Fig. 4, B and F). The often considerably enlarged terminals are consistent with our ultrastructural observations for both TNT expression and loss of *n-syb* and were not observed for *v100*. All markers of the endolysosomal system analyzed here were significantly up-regulated, including Syx7, Rab5, Rab7, and Hrs (Fig. 4, C, D, and G; and Fig. 5, A and E). The transmembrane receptor Fas2, which we have previously shown is strongly up-regulated in *n-syb* photoreceptors (Hiesinger et al., 1999), colocalizes evenly to Syx7 in the enlarged *n-syb* terminals, suggesting that Fas2 accumulates on Syx7-positive endosomal vesicles (Fig. 4 B). The up-regulation of endosomal markers was further verified with immunoblot analysis of protein extract from complete eyes for Syx7 and Hrs (Fig. 4 H). In contrast

YFP-Rab7 (E), and YFP-Rab11 (F) expression with n-Syb antibody. Single YFP channels are shown in (D′–F′). All arrows show compartments with colocalization, and arrowheads indicate lack of colocalization. (G–H′′′′) High-resolution single sections from deconvolved 3D confocal datasets (Hiesinger et al., 2001). Note that individual compartments are discernible both in the cell body (cb) region and at synapses (syn) that are positive for various combinations of endosomal markers: n-Syb, V100, Syx7, and Rab5 (green in H). Original sections are shown in G and H, deconvolved sections are shown in G′ and H′, and single channels are shown in G′′–G′′′′ and H′′–H′′′′. Bars: (C–E and G) 5 µm; (H) 2 µm. All error bars are SEM. WT, wild type.

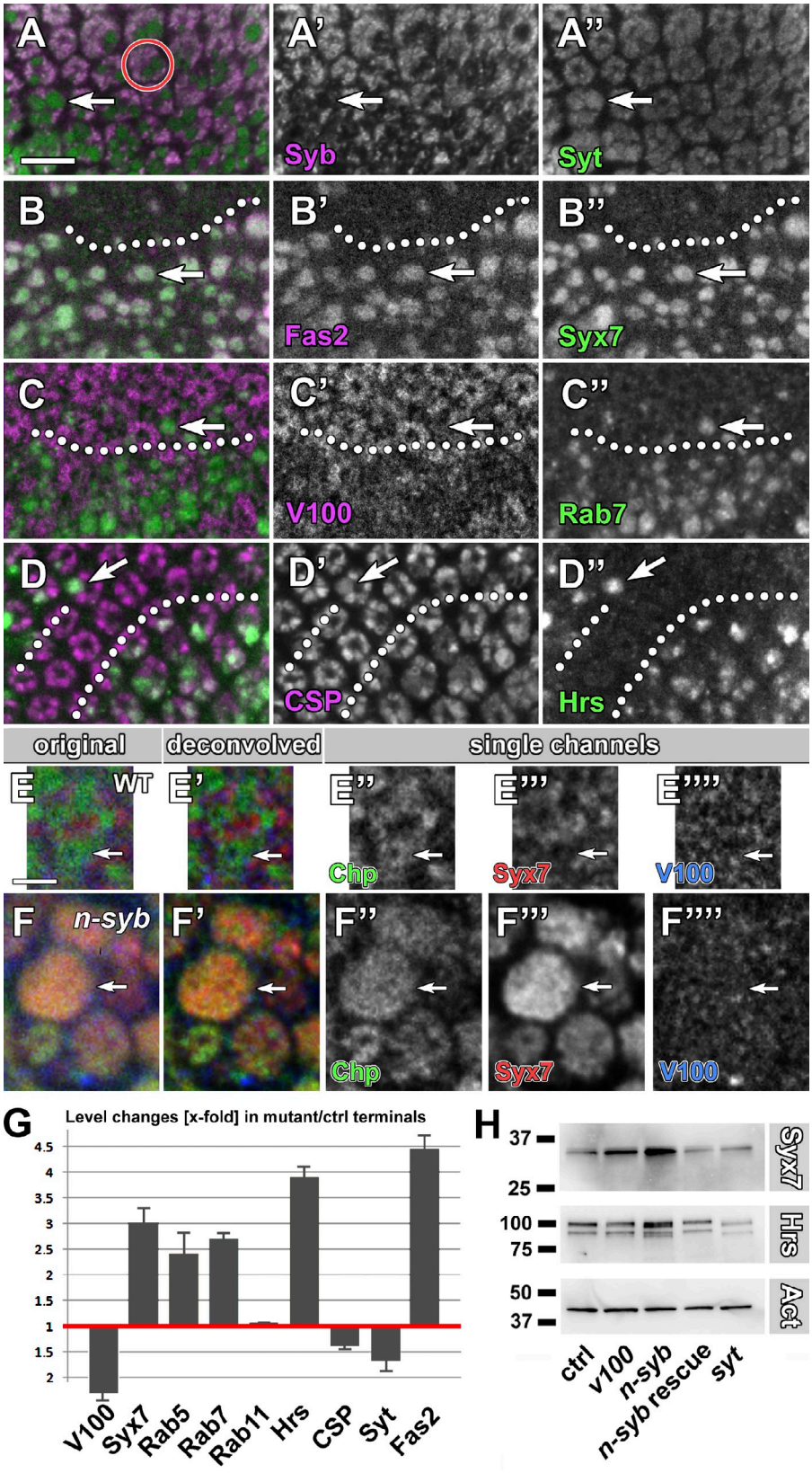

Figure 4. **Loss of *n-syb* causes accumulations of endosomal markers.** (A–D′′) Lamina cross sections of 1-d-old flies showing the structure of adult cartridges in 50% photoreceptor-specific genetic mosaics. (A) Immunolabeling for n-Syb and Syt. (B) Fas2 and Syx7. (C) V100 and Rab7. (D) CSP and Hrs. Single channels are shown in A′–D′′. Approximate clonal boundaries are indicated with dotted lines in B–D. (E–F′′′′) Single cartridge (circle in A) in high-resolution single sections from original and deconvolved 3D confocal datasets for control (E) and *n-syb* (F). Originals are shown in E and F, deconvolved sections are shown in E′ and F′, and single channels are shown in E′′–E′′′′ and F′′–F′′′′. Chaoptin (Chp), Syx7, and V100. Note that individual *n-syb* mutant photoreceptor terminals can reach the diameter of a complete wild-type cartridge profile and are evenly filled with Chaoptin and Syx7. (G) Ratio of expression levels in mutant photoreceptor terminals compared with wild-type control in 50% mutant mosaics as shown in A–D. (H) Western blot analysis of *n-syb* mutant eyes. Bars: (A) 10 µm; (E) 5 µm. Arrows show individual enlarged terminals. Error bars are SEM (n = 3 laminae). Molecular markers are given in kilodaltons. ctrl, control.

to endolysosomal proteins, synaptic vesicle markers were unaltered or slightly down-regulated, similar to observations previously made for *v100* mutant photoreceptor terminals (Fig. 4 G; Williamson et al., 2010a). Interestingly, V100 itself is mostly lost at *n-syb* mutant synapses (Fig. 4 C). These findings suggest that the accumulated vesicles observed in *n-syb* mutant terminals with EM do not represent either synaptic vesicles or vesicles lacking the normal complement of synaptic vesicle proteins.

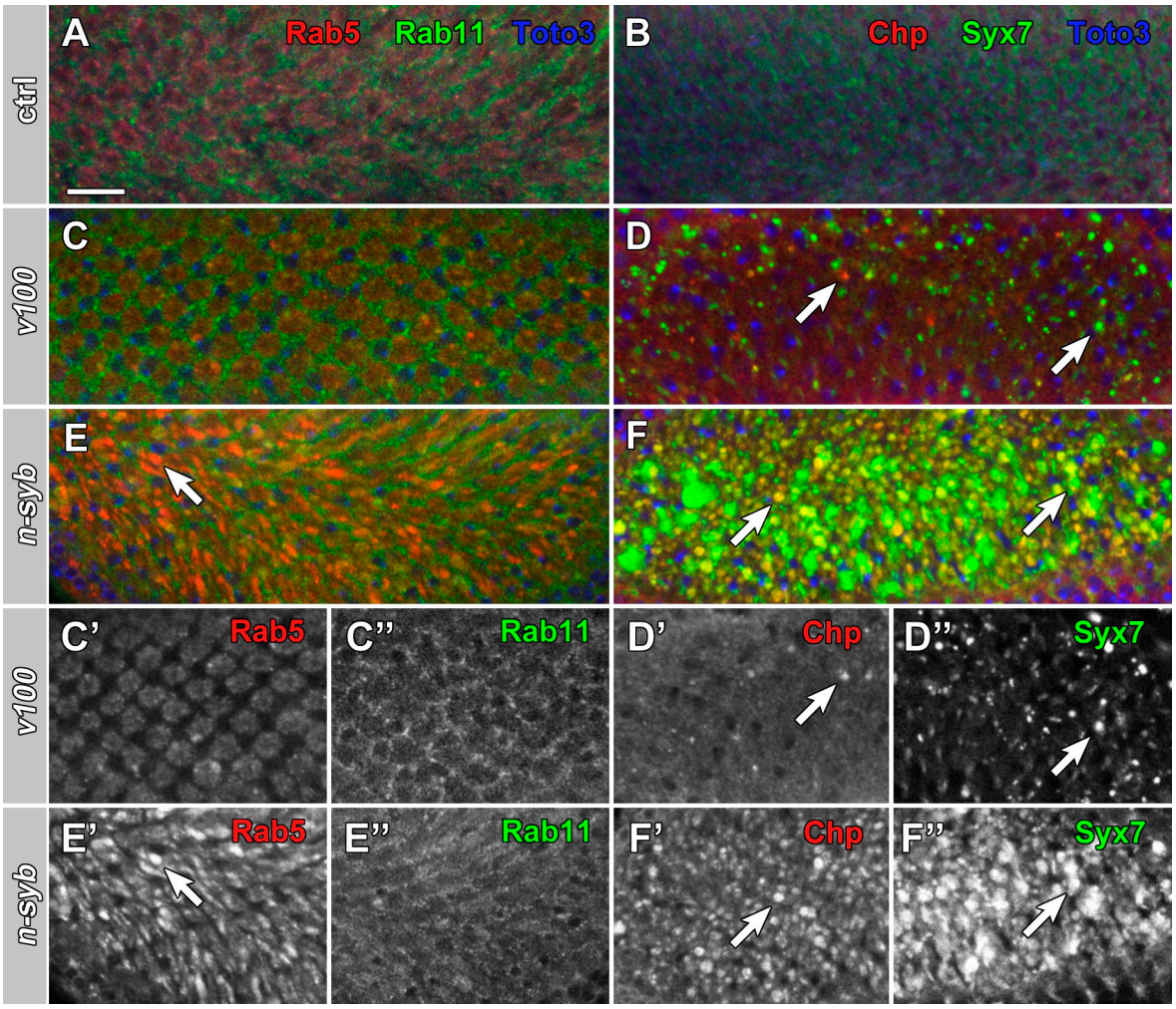

Figure 5. ***n-syb* mutant synapses exhibit more endosomal accumulations than *v100*.** (A and B) 1-d-old wild-type lamina cross sections immunolabeled for Rab5, Rab11, and Toto3 (A) or Chaoptin, Syx7, and Toto3 (B). (C and D) *v100* mutant photoreceptor terminals exhibit distinct accumulations of the early endosomal markers Rab5, Syx7, and the transmembrane receptor Chaoptin. (E and F) *n-syb* mutant photoreceptor terminals exhibit substantially more endosomal accumulations, especially Syx7. Single channels for half panels are shown in C′–F′. Arrows indicate individual endosomal accumulations not observed in the control. Bar, 10 µm.

Many enlarged *n-syb* mutant terminals have a diameter of 5 µm or more, large enough to permit an analysis of the subcellular distribution of intracellular compartment markers. As shown in Fig. 4 (E and F) with high-resolution sections from 3D deconvolved confocal datasets, such enlarged terminals appear evenly filled with Syx7 and the photoreceptor-specific transmembrane receptor Chaoptin (Krantz and Zipursky, 1990), which is not observed in wild type. Hence, membrane receptors, including Fas2 (Fig. 4 B) and Chaoptin (Fig. 4 F), exhibit a distribution and colocalization to early endosomal markers that suggest accumulation of large numbers of endosomal vesicles that evenly fill *n-syb* terminals. Because the loss of *n-syb* caused no obvious defects in eye development, cell type specification, or axon pathfinding, we infer that spatiotemporally regulated exo- and endocytosis of developmentally required receptors do not require *n-syb*. In contrast, loss of *syx7* causes early developmental and tumor growth phenotypes not observed in the *n-syb* mutant (Lu and Bilder, 2005), and n-Syb does not directly interact with Syx7 (Fig. S4 A; Antonin et al., 2000) but may reside on the same endocytic vesicles, as suggested by the wild-type colocalization. Collectively with the wild-type localization data, these observations suggest that n-Syb has a hitherto unrecognized function in endolysosomal progression.

Next, we directly compared the endosomal defects in *n-syb* and *v100* mutant synaptic terminals. Immunolabeling of whole laminae reveals that synaptic accumulations of the early endosomal proteins Rab5 (Fig. 5, A, C, and E) and Syx7 (Fig. 5, B, D, and F) are substantially increased in *n-syb* compared with *v100*. In contrast, the recycling endosomal marker Rab11 is not noticeably altered in either mutant. Interestingly, degeneration is more severe in the *v100* mutants (Fig. 1), yet the endosomal accumulations and swelling of photoreceptor terminals are considerably more severe in the *n-syb* mutant. These findings suggest that the severity of degeneration depends on the type of endolysosomal defect and is not simply a function of the amount of endosomal vesicle accumulation.

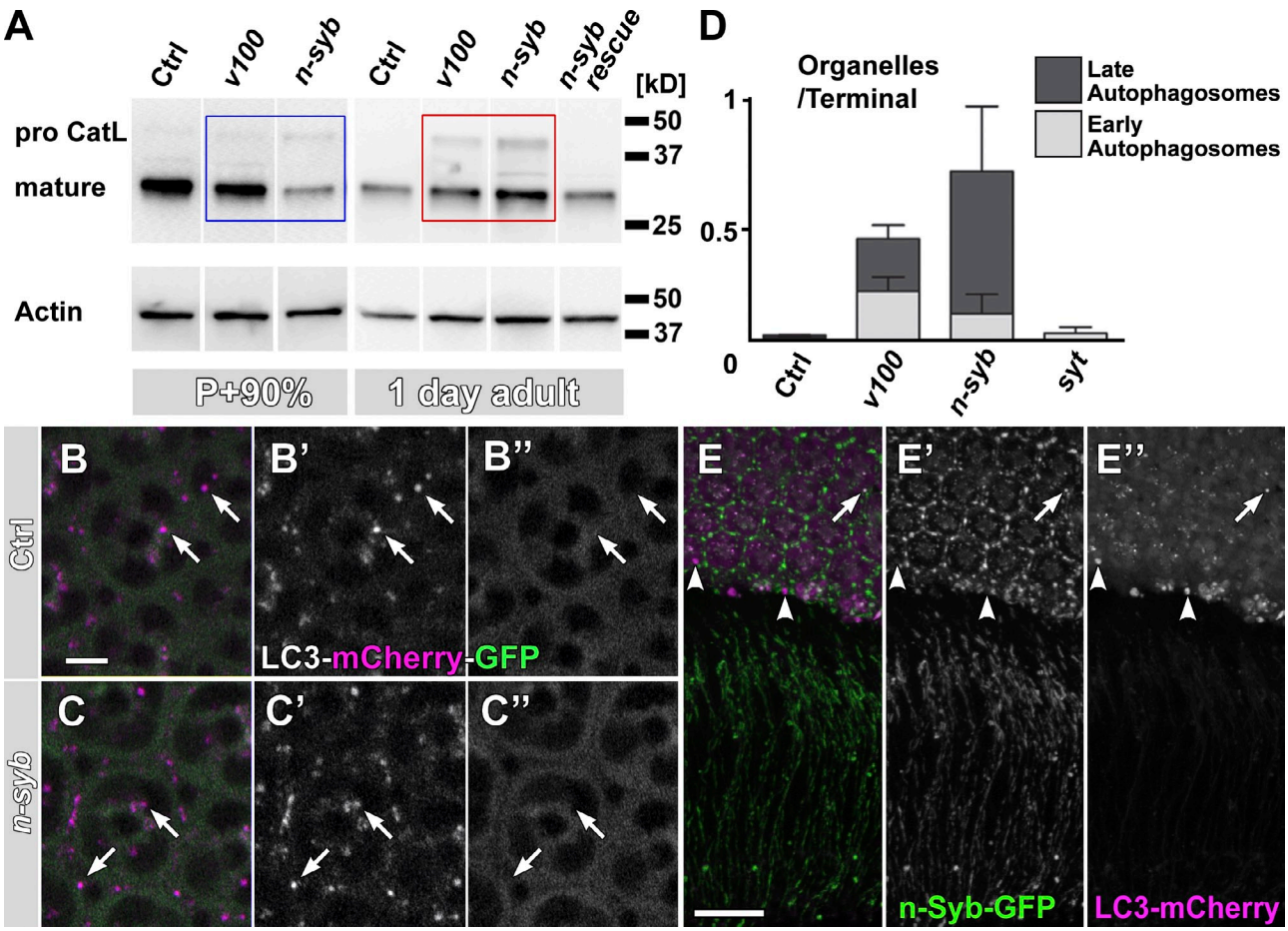

Figure 6. **Loss of *n-syb* causes a primary defect in delivering degradation machinery vesicles to to-be-degraded compartments.** (A) Western blot analysis of mutant eyes (*n-syb* and *v100*) at P+90% and 1 d after eclosion, probed with an antibody against insect Cathepsin L (CatL). Note that at P+90%, mature Cathepsin is reduced in *n-syb* compared with control and *v100* (blue box) but increased in the adult (red box). (B and C) Live imaging of the Atg8/LC3-mCherry-GFP fusion reporter in wild-type (B) and *n-syb* (C) photoreceptors. Note that GFP fluorescence, but not mCherry fluorescence, is quenched in an acidification-dependent manner (arrows). (D) Profile counts of early and late autophagosomes based on EM. Examples are shown in Fig. S4. (E) Wild-type cooverexpression of GFP–*n-syb* and LC3/Atg8-mCherry reveals little colocalization (arrow), large autophagosomes that are n-Syb negative (arrowheads), and no autophagosomes at synapses in wild type. Bars: (B) 5 µm; (E) 10 µm. All error bars are SEM. Ctrl, control.

Loss of *n-syb* causes a primary defect in delivering degradation machinery vesicles to endosomal compartments

What intracellular membrane fusion reaction is disrupted by loss of *n-syb*? Because loss of *n-syb* leads to a failure to degrade heterogeneous endosomal, multivesicular, and autophagosomal compartments in a manner reminiscent of loss of *v100*, a possible explanation is a failure to deliver proteins required for degradation. Such Golgi-derived degradation machinery vesicles might contain the v-ATPase, including V100, as well as lysosomal proteases.

Cathepsins are lysosomal proteases that are synthesized in the endoplasmic reticulum as an inactive, high molecular weight proform that is activated by proteolytic cleavage only in strongly acidified compartments (Lee et al., 2010). The acidification-dependent proteolytic cleavage of pro-Cathepsins generates mature Cathepsins of low molecular weight that can be readily distinguished from the larger proform on Western blots. Hence, analysis of the ratio between the proform and mature Cathepsin provides a means to assay whether vesicles containing degradative enzymes can fuse with lysosomal and autophagosomal compartments. As shown in Fig. 6 A, an antibody against insect Cathepsin L detects a single band of the mature form at 30 kD in protein extract from wild-type eyes. Loss of *n-syb* resulted in the appearance of a high molecular proform that is not detectable in protein extract from control eyes of 1-d-old flies (Fig. 6 A, red box). Interestingly, the accumulation of pro-Cathepsin in *n-syb* was more pronounced than in *v100* or two other degradation mutants, the lysosomal tetraspanin *sunglasses* or the lysosomal sugar transporter *benchwarmer/spinster* (Fig. S4 B; Sweeney and Davis, 2002; Xu et al., 2004; Dermaut et al., 2005). These findings are consistent with the idea of a delivery defect of pro-Cathepsin–containing vesicles in the *n-syb* mutant.

Is the delivery of pro-Cathepsin vesicle a primary defect in the *n-syb* mutant? In addition to the increase in pro-Cathepsin, we found that mature Cathepsin L, which was robustly present in wild type, also exhibited a significant increase that is most pronounced in *n-syb*. This is surprising because it implies that more Cathepsin accumulated in both nonacidified (pro-Cathepsin) as well as acidified (mature Cathepsin) compartments. We therefore examined which defect occurs first, the

failed delivery of pro-Cathepsin vesicles or the accumulation of mature Cathepsin in degradative compartments. Interestingly, *n-syb* mutant eyes from late pupae (P+90%) already exhibited a mild increase in pro-Cathepsin but a temporary decrease of mature Cathepsin, consistent with an initial failure to deliver Cathepsin vesicles to degradative compartments (Fig. 6 A, blue box). These phenotypes differ from V100, which also showed an increase of pro-Cathepsin (albeit less than in *n-syb*) at 1 d after eclosion but not at P+90%, consistent with our previous analyses (Fig. 6 A; Williamson et al., 2010a). We conclude that the accumulation of pro-Cathepsin precedes the increase of mature Cathepsin in *n-syb*, supporting the hypothesis that delivery of pro-Cathepsin–containing vesicles is a primary defect. This interpretation is further supported by the EM of developing photoreceptor terminals lacking functional n-Syb in which the accumulation of small vesicles precedes the appearance of larger compartments (Fig. S3).

Because both autophagosomes and the increase in mature Cathepsin only appear in the adult mutant (Fig. 6 A and Fig. S3), we set out to test the possibility that autophagy is a secondary response to an earlier trafficking defect caused by loss of *n-syb*. Autophagy is critically important for neuronal maintenance (Hara et al., 2006; Komatsu et al., 2006), but autophagy is not known to require any neuron-specific proteins. A recently developed probe to measure autophagosome acidification is based on the autophagosome marker Atg8/LC3; double tagging with acidification-sensitive GFP and acidification-insensitive mCherry leads to selective quenching of GFP of this reporter only in acidified autophagosomes (Filimonenko et al., 2007). As shown in Fig. 6 (B and C), autophagosomes in wild-type and *n-syb* mutant photoreceptor cell bodies exhibited selective quenching of GFP, indicating that they were indeed acidified. Furthermore, if these autophagosomal compartments contained active proteases, we should observe morphologically distinct, late-stage autophagosomes with degraded contents. We therefore counted early stage autophagosome profiles (immature autophagosomal vacuoles [AVIs]; containing large, morphologically recognizable cellular structures; Fig. S5, arrowheads) and late autophagosome profiles (degradative autophagosomal vacuoloes [AVDs]; containing only small, electron-dense debris; Fig. S5, arrows). These counts revealed that almost 90% of all autophagosomes in the *n-syb* mutant are late AVDs, whereas AVI and AVD profiles appeared in a 50:50 ratio in *v100* mutants, which are predicted to partially lack acidification required for degradation (Fig. S5). Finally, cooverexpression of tagged versions of the autophagosome markers LC3/Atg8 and n-Syb revealed that autophagosomes are primarily found in cell bodies, where they only partially overlap with n-Syb. In contrast, n-Syb is transported to the synapses and in the cell bodies marked mostly compartments that are not positive for LC3/Atg8 (Fig. 6 E). This nonoverlapping pattern of expression further supports an autophagy-independent function of n-Syb. We conclude that by all the criteria we have investigated here, autophagy seems to be functional until late stages of autophagosome maturation independent of *n-syb* and that the pronounced increases in endosomal markers and vesicles are distinct from the increase in the number of autophagosomes. The presence of autophagosomal accumulations may reflect a dramatic increase of functional autophagy, or loss of *n-syb* causes a defect in removing late autophagosomal compartments. In both scenarios, increased autophagy is likely to be a secondary response to a primary vesicle trafficking defect downstream of endocytosis.

Early cell death through induction of autophagy or *tau* overexpression does not depend on *n-syb*, but loss of *n-syb* sensitizes adult photoreceptors to degeneration

Unchecked induction of autophagy through overexpression of *atg1* causes cell death (Berry and Baehrecke, 2007; Scott et al., 2007). Correspondingly, high levels of *atg1* overexpression during photoreceptor development cause eye developmental defects that result in a reduced and rough eye (Fig. 7, A and E). *atg1*-induced cell death thus provides a direct test as to whether *n-syb* is required for autophagy in photoreceptors. As shown in Fig. 7 (E and F), loss of *n-syb* did not reduce the ability of *atg1*-induced autophagy to disrupt eye development. Interestingly, loss of *n-syb* did not noticeably increase the developmental defect as indicated by indistinguishable reductions in eye size. However, ERG recordings from these eyes in 1-d-old flies revealed a reduced response amplitude in *atg1*-overexpressing photoreceptors that was further reduced in an *n-syb* mutant background. These findings indicate that *n-syb* is not required for *atg1*-induced autophagy but has an additive negative effect on adult photoreceptor function. The genetics therefore do not indicate a requirement of *n-syb* for autophagy but rather suggest that loss of *n-syb* sensitizes adult photoreceptors to neurotoxic insults through an independent mechanism. To test this idea further, we challenged wild-type and *n-syb* mutant photoreceptors with overexpression of human *tau* protein, similar to an experiment recently performed for *v100* (Wittmann et al., 2001; Williamson and Hiesinger, 2010a). Overexpression of *tau* caused a defective eye morphology and reduction of the ERG response amplitude similar in strength to *atg1* overexpression (Fig. 7, I–L). As in the case of *atg1* overexpression, loss of *n-syb* did not noticeably affect the developmental defect but lead to a further reduction of the response amplitude in the adult (Fig. 7, K and L). We conclude that impaired intracellular degradation through loss of *n-syb* sensitizes adult photoreceptor neurons to neurotoxic insults and that *n-syb* is not required for *atg1*-induced autophagy.

Overexpression of V100 partially rescues *n-syb*–dependent neurodegeneration

Loss of either *n-syb* or *v100* causes synaptic dysfunction, neurodegeneration, and accumulation of undegraded endosomal compartments. Furthermore, loss of *n-syb* leads to reduced V100 localization at synapses. To test genetic interactions between the two mutants, we analyzed both RNAi-mediated loss of *v100* (Williamson and Hiesinger, 2010a) and *v100* overexpression in *n-syb* mutant photoreceptors. *v100* RNAi does not rescue *n-syb*–dependent degeneration (unpublished data). In contrast, overexpressing V100 partially rescues both

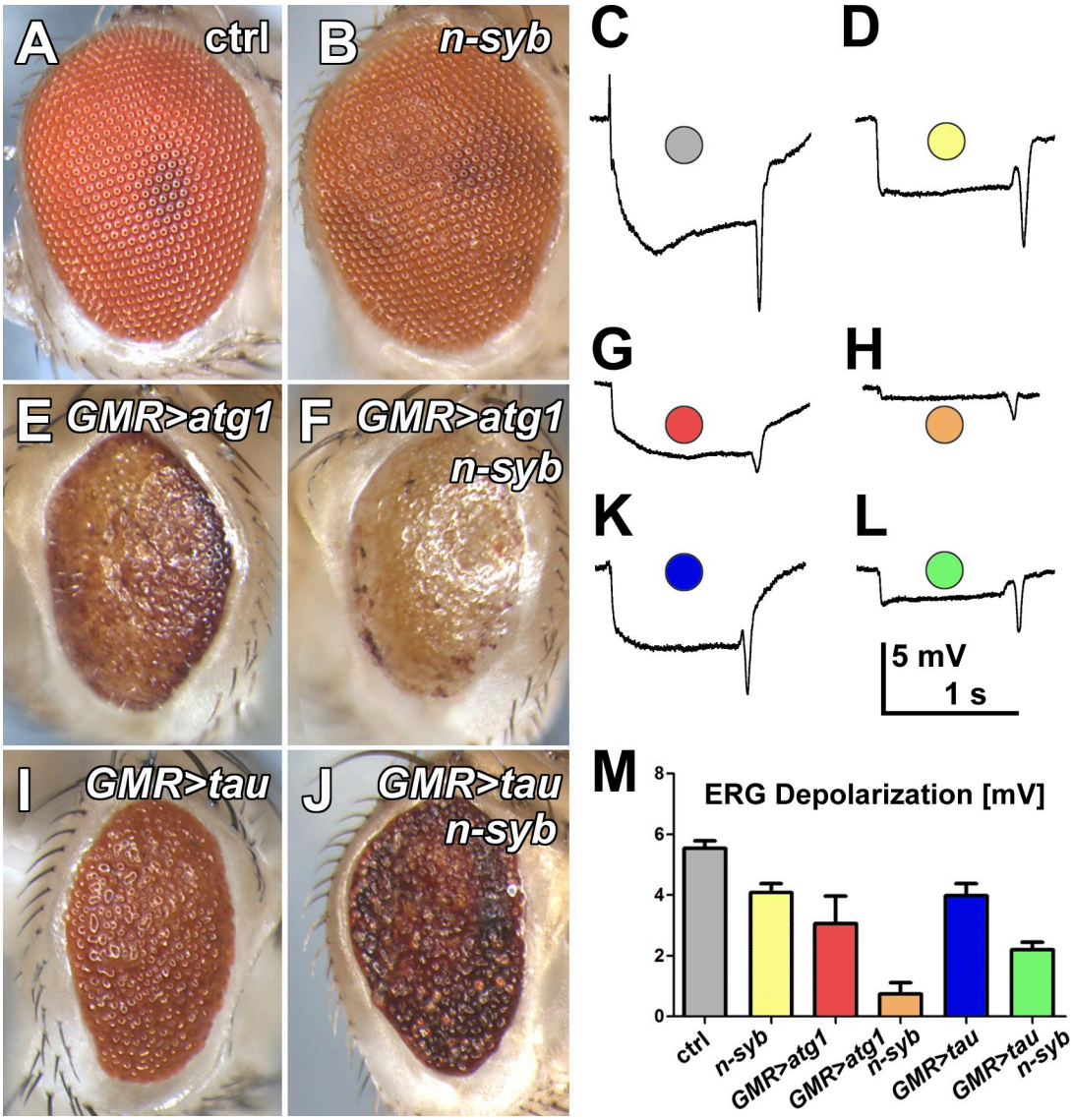

Figure 7. **Early cell death through induction of autophagy or *tau* overexpression does not depend on *n-syb*, but loss of *n-syb* sensitizes adult photoreceptors to degeneration.** (A–L) Eye pictures and sample ERG traces for control (A and C), n-syb (B and D), autophagy induction through *atg1* expression in wild type (E and G), and *n-syb* mutant (F and H) photoreceptors. Expression of human *tau* in wild-type (I and K) and mutant (J and L) photoreceptors. (M) Quantification of ERG response amplitudes. Note that loss of *n-syb* does not obviously alter the developmental eye defects but leads to further reduced response amplitudes in adult photoreceptors. All error bars are SEM. ctrl, control.

morphological and functional degeneration (Fig. 8). We undertook ERG and immunohistochemical analyses in flies that had been exposed to constant light for 7 d. Under these conditions, wild-type photoreceptors exhibited both a normal ERG and morphology (Fig. 8, A and E). In contrast, *n-syb* mutant photoreceptors exhibited a significant reduction in the number of rhabdomere profiles (Fig. 8 B) and an ∼50% reduction of depolarization (Fig. 8, F and J). Photoreceptor-specific expression of *v100* in the *n-syb* mutant terminals partially but significantly rescued the defect in rhabdomere number (Fig. 8, C and K) as well as ERG depolarization (Fig. 8, G and J). Next, we tested whether the acidification function of V100 is required for this rescue. We have previously generated the $v100^{R755A}$ mutant that selectively disrupts proton translocation (Williamson et al., 2010a). Surprisingly, $v100^{R755A}$ expression in photoreceptors rescued the degeneration defect to an extent indistinguishable from wild-type *v100* overexpression. Note that the loss of neurotransmitter release (as measured by the ERG "on" transient) in *n-syb* mutant neurons was not rescued by either wild-type or acidification-defective *v100* (Fig. 8 I). Our results indicate that the acidification-independent function of V100 is sufficient to significantly protect *n-syb* mutant photoreceptor neurons from degeneration independent of neurotransmitter release.

V100 overexpression does not reduce intracellular accumulations but increases undegraded cargo colocalization with early endosomes

The rescue with acidification-defective $v100^{R755A}$ is not consistent with increased degradation as a rescuing parameter. To the contrary, we found even more widespread and evenly

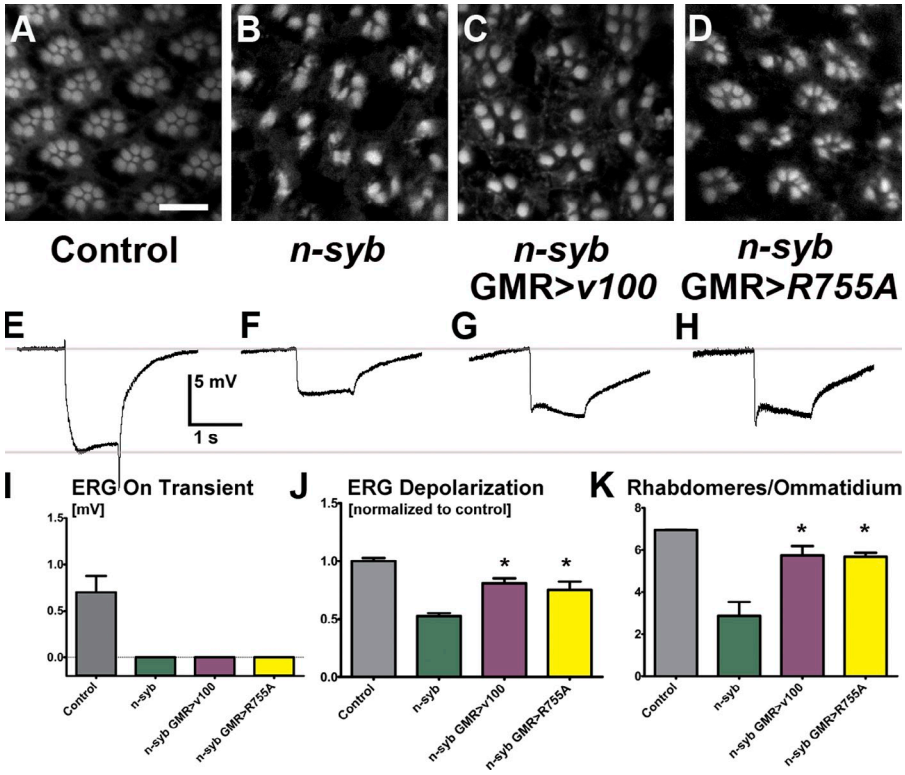

Figure 8. **Overexpression of V100 partially rescues *n-syb*–dependent neurodegeneration.** (A–D) Rhabdomere counts as shown in Fig. 1 (A–E) for wild type (A), *n-syb* (B), photoreceptor-specific expression of *v100* in *n-syb* (C), and expression of the acidification-defective $v100^{R755A}$ in *n-syb* (D). (E–H) ERG photoreceptor depolarization magnitudes as shown in Fig. 1 (F–J) for the genotypes shown in A–D. (I) Magnitude of ERG "on" transients reveals lack of rescue of neurotransmission at photoreceptor synapse. (J) Magnitude of ERG depolarization reveals rescue of photoreceptor responses to light stimuli. (K) Counts of rhabdomere degeneration. Bar, 10 µm. All error bars are SEM. *, $P < 0.05$.

distributed Syx7 immunoreactivity for both *v100*- and $v100^{R755A}$-expressing *n-syb* mutant cells compared with *n-syb* mutants (Fig. 9, A–D, compare arrows with arrowheads). This subcellular distribution is suggestive of large numbers of small endosomal vesicles rather than large and distinct endolysosomal or autophagosomal compartments. Colabeling of Rhodopsin 1, a heavily trafficked and recycled receptor in photoreceptor cell bodies, exhibited increased colocalization with the evenly distributed cytoplasmic Syx7 labeling for both *v100* and $v100^{R755A}$ rescue (Fig. 9, arrows) compared with *n-syb* (Fig. 9, arrowheads). These observations do not indicate any obvious rescue of endosomal accumulations but rather suggest a subtle redistribution of subcellular endosomal compartments and receptor cargo upon V100 overexpression. Furthermore, high-resolution scans of *n-syb*–null synaptic terminals overexpressing *v100* revealed substantial terminal size increases and endolysosomal protein accumulations that were very similar to the *n-syb* mutant (Fig. 9, E–J). Quantification of early and late endosomal markers revealed no significant change of Syx7 but a small reduction of the late endosomal marker Rab7 at synaptic terminals (Fig. 9, E–H). In addition, the most obvious difference at the synapses of V100-overexpressing *n-syb* mutant neurons was a restoration of the localization of V100 itself to synapses where it is evenly distributed (i.e., in small vesicles) rather than in distinguishable large compartments (i.e., autophagosomes; Fig. 9, I and J). In summary, we found no rescue of the endosomal accumulations or degradation defects by *v100* or $v100^{R755A}$ overexpression but rather a further increase in cargo colocalization to compartments labeled with early endosomal markers both in the cell body and at synapses.

We next asked how Cathepsin sorting and processing is affected by *v100* overexpression in *n-syb* mutant photoreceptors. As shown in Fig. 9 K, overexpression of *v100* in *n-syb* mutant photoreceptors caused a further increase of both pro-Cathepsin and mature Cathepsin, whereas overexpression of *v100* in wild-type photoreceptors caused only very mild changes. This result suggests that some Cathepsin was normally degraded independent of *n-syb* but now rerouted by V100.

Based on the *v100* overexpression results, we hypothesized that V100 is a component of Cathepsin-containing vesicles and that it plays a role during vesicle sorting (Fig. 10). As shown in Fig. 9 K, expression of $v100^{R755A}$ in the *n-syb* mutant lead to a substantial increase in pro-Cathepsin at the expense of mature Cathepsin. This observation strongly supports the idea that the overexpressed V100 indeed resides on vesicles that contain Cathepsin and that the vesicles require V100's acidification function to mature. Note that expressing the acidification-defective $v100^{R755A}$ only had a very mild effect in wild-type neurons, whereas its expression in *n-syb* mutant, alone among all genotypes analyzed here, lead to a ratio reversal to more pro- than mature Cathepsin (Fig. 9 K). Furthermore, $v100^{R755A}$ expression in the *n-syb* mutant decreased mature Cathepsin when compared with the *n-syb* mutant alone. Because expression of $V100^{R755A}$ rescues degeneration to the same extent as wild-type *v100*, these findings are not consistent with increased degradative capacity as a rescuing parameter. Instead, the $V100^{R755A}$ experiment suggests that V100 reroutes Cathepsin vesicles to compartments for whose acidification V100 itself is required. Finally, we observe that the further increase of cargo colocalization with early endosomal compartments in these rescue experiments coincides with reduced neurodegeneration compared with the *n-syb* mutant.

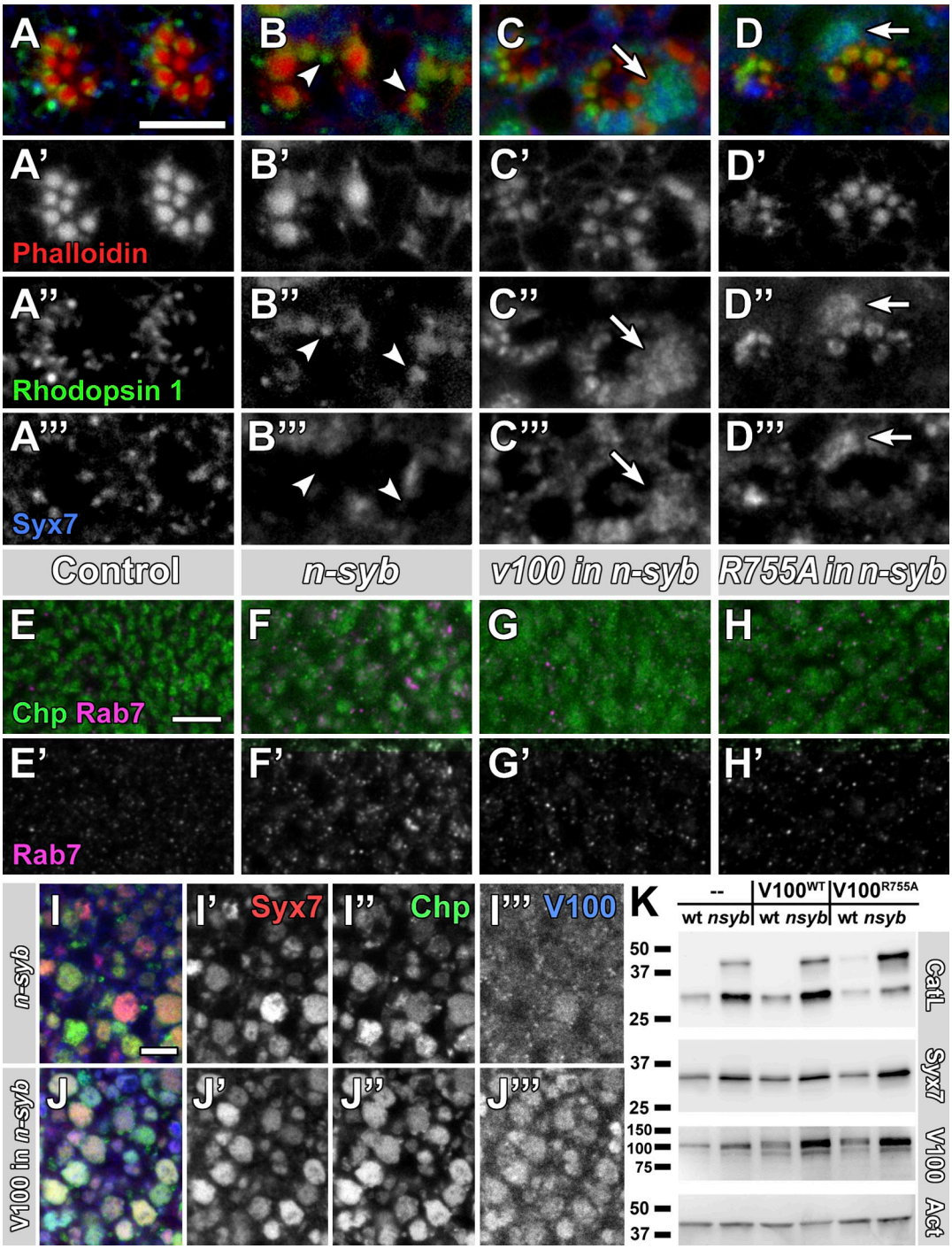

Figure 9. **V100 overexpression does not reduce intracellular accumulations but increases undegraded cargo colocalization with early endosomes.** (A–D′′′) High-resolution images of ommatidia and rhabdomeres for wild-type (A), *n-syb* (B), photoreceptor-specific expressing *v100* in *n-syb* (C), and acidification-defective v100^{R755A} expressing in n-*syb* (D). Single channels are shown in A′–D′′′. Arrows indicate Syx7/Rhodopsin colocalization; arrowheads indicate absence of Rhodopsin 1/Syx7 colocalization. (E–H) Lamina cross sections with photoreceptor terminals for the same genotypes as in A–D. (I and J) High-resolution lamina cross sections of photoreceptor terminals for *n-syb* (I) and *v100* overexpression in *n-syb* (J). Single channels shown in I′–J′′′. (K) Western blot analysis of mutant eyes for the genotypes indicated. (top) Cathepsin L (CatL); (middle) Syx7; (bottom) V100 and Actin (Act). Bars: (A and E) 10 µm; (I) 5 µm. Molecular markers are given in kilodaltons. Chp, Chaoptin.

Similarly, the *n-syb* mutant exhibits increased endosomal accumulation and reduced neurodegeneration compared with *v100*. Based on these observations, we speculate that early endosomal compartments are less toxic for the cell than accumulations of late endosomal/degradative compartments.

Discussion

We have characterized an unexpected function of the neuronal v-SNARE n-Syb in endolysosomal trafficking that is independent of its known function in neurotransmitter release. Loss of

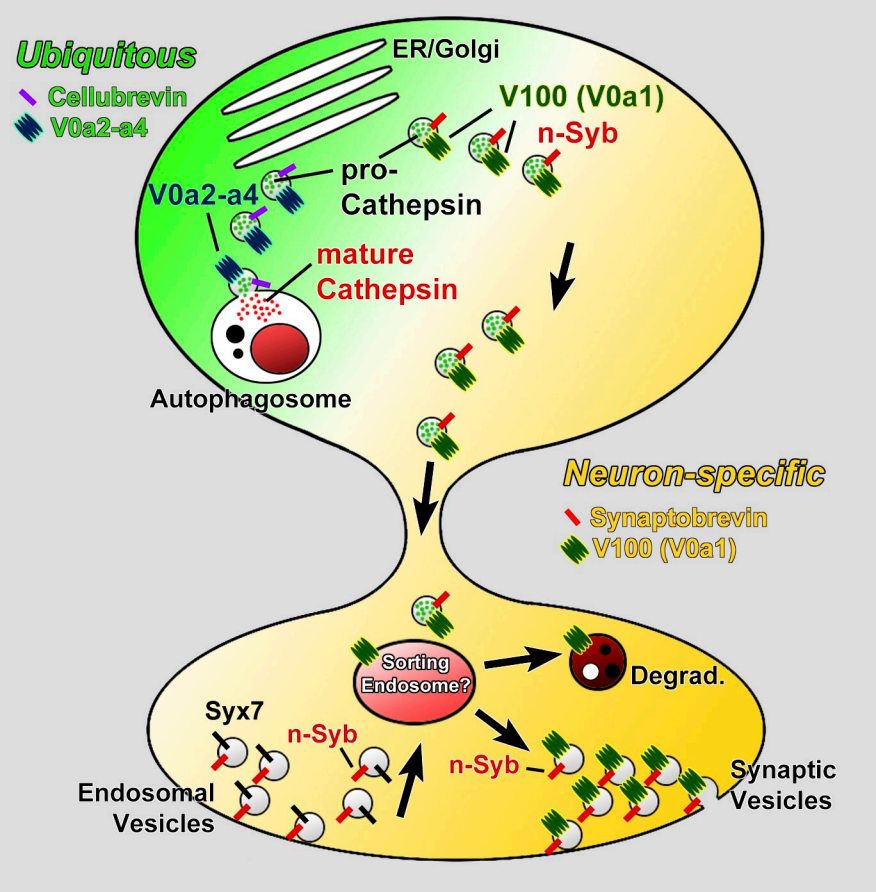

Figure 10. **n-Syb and V100 are part of a neuron-specific sort-and-degrade mechanism that functions in parallel to ubiquitous endolysosomal and autophagosomal degradation.** Schematic of a neuronal cell body (top) and synaptic terminal (bottom) with ubiquitous sorting and degradation (Degrad.) machinery shown on green background and neuron-specific machinery shown on yellow background. Autophagosome formation and function are part of the ubiquitous machinery and independent of *n-syb*. Loss of *n-syb* results in a failure to fuse neuron-specific V100/Cathepsin-containing vesicles with endosomal compartments. Loss of either *n-syb* or *v100* causes the loss of only a neuronal subset of degradative compartments, as indicated by the persistence of mature Cathepsin in both mutants. Although early development, including cell type specification, does not depend on the neuron-specific sort-and-degrade mechanism, loss of either *n-syb* or *v100* causes endolysosomal protein accumulations and progressive neurodegeneration.

this function leads to neurodegeneration in adult fly photoreceptor neurons. These findings explain our earlier observations of late developmental defects during brain wiring that do not occur when neuronal activity or neurotransmitter release is impaired (Hiesinger et al., 1999, 2006). Genetic and cell biological evidence indicates that n-Syb functions in concert with the neuronal v-ATPase component V100 in a neuronal sort and degrade pathway. Specifically, our evidence supports a primary defect in the fusion of vesicles that contain degradation machinery (including degradation proteases and V100-containing ATPases required to activate them) with endosomal compartments.

A role in neuronal vesicle fusion independent of synaptic vesicle exocytosis

The ultrastructure of *n-syb* mutant terminals reveals accumulations of both small vesicles and large degradative and autophagosomal compartments. n-Syb is a small (<200 amino acids) protein that is very well characterized as a synaptic v-SNARE required for vesicle fusion (Broadie et al., 1995; Galli et al., 1995; Deitcher et al., 1998; Südhof and Rothman, 2009). In addition, synaptic vesicles are sorted through synaptic endosomes (Uytterhoeven et al., 2011). Hence, the most straightforward explanation for endolysosomal trafficking defects in *n-syb* mutant neurons would be a defect in vesicle fusion.

Several observations indicate that the endolysosomal defect is not directly linked to n-Syb's function in synaptic vesicle exocytosis. First, loss of neuronal activity or neurotransmitter release does not cause endolysosomal, developmental or degenerative phenotypes in *Drosophila* photoreceptors as shown here and previously (Hiesinger et al., 2006). Second, although vesicles accumulate, synaptic vesicle markers do not accumulate correspondingly. Instead, we find that several markers of the endolysosomal system are up-regulated. In particular, the early endosomal t-SNARE Syx7, together with transmembrane receptors, including Chaoptin and Fasciclin 2, exhibits a strong up-regulation and evenly fills the profiles of enlarged synaptic terminals. Together with the EM data, we conclude that synaptic terminals are filled with large numbers of endosomal vesicles rather than with synaptic vesicles.

Several lines of evidence indicate that *n-syb* is not required for autophagosome maturation, at least up to a late stage. First, n-Syb colocalizes only little with autophagosomes but marks mostly endosomal compartments and synaptic vesicles. Second, autophagosomes are acidified and contain active proteases (Cathepsins) and degraded material based on EM, Atg8-mCherry-GFP measurements, and mature Cathepsin accumulations. Third, induction of autophagy by *atg1* expression does not depend on *n-syb*. Finally, the accumulation of undegraded Chaoptin and Fasciclin 2 receptors that evenly fill terminals is not consistent with their accumulation in autophagosomes. Because autophagy typically initiates in response to nutrient deprivation or other neurotoxic insults, the appearance of autophagosomes may be a secondary response (Tooze and Schiavo, 2008; McPhee and Baehrecke, 2009).

What then is n-Syb's other vesicle fusion role? We have evidence for at least two types of small vesicles accumulating in *n-syb* terminals: small endosomal vesicles and Cathepsin-containing ER/Golgi-derived transport vesicles. The early accumulation of pro-Cathepsin–containing vesicles suggests a defect in vesicle fusion and is not easily explained by defective exocytosis at the plasma membrane. Importantly, our observations show that most intracellular vesicle fusion events are unaffected by loss of *n-syb*, consistent with the presence and partially redundant function of the ubiquitous v-SNARE Cellubrevin in photoreceptors (Bhattacharya et al., 2002). Most prominently, the complete absence of any early developmental defect implies that *n-syb* cannot be required for the canonical secretory pathway that regulates morphogen and receptor exocytosis. Similarly, spatiotemporally regulated receptor endocytosis appears unaffected because receptor accumulations distribute evenly in the enlarged *n-syb* mutant terminals. We conclude that receptors accumulate in small endocytic vesicles downstream of endocytosis and upstream of further sorting or degradation. Collectively, these observations pinpoint a role for n-Syb in the fusion of Cathepsin/V100-containing (degradation machinery) vesicles with to-be-degraded compartments (Fig. 10). The latter do not include autophagosomes, as Cathepsin delivery to autophagosomes is apparently unimpaired. Furthermore, the large numbers of Syx7-positive small endosomal vesicles are not likely a fusion partner because Syx7 does not directly interact with n-Syb as shown here and in vertebrates (Antonin et al., 2000). Instead, we can narrow down the function to a fusion reaction between V100/Cathepsin degradation machinery vesicles with neuronal endolysosomal compartments before the formation of lysosomes. The n-Syb–mediated endolysosomal fusion event could be directly between degradation machinery vesicles and larger or intermediate endosomal vesicles or sorting compartments, with which fusion of small endosomal vesicles is also blocked in the absence of *n-syb* (Fig. 10). In either case, the intravesicular endosomal fusion uncovered by loss of *n-syb* represents a neuronal specialization and possible addition to the ubiquitous endolysosomal machinery, as shown in the model in Fig. 10.

A neuronal sort-and-degrade mechanism and its implications for neurodegeneration

We recently reported that the neuron-specific v-ATPase component V100 defines a neuronal sort-and-degrade mechanism that increases neuronal degradative capacity (Williamson and Hiesinger, 2010a; Williamson et al., 2010a). Loss of *n-syb* and *v100* reveals striking similarities with one remarkable difference: endosomal accumulations in *n-syb* are considerably more severe and lead to a several-fold enlargement of synaptic terminals and yet a significantly slower progression of degeneration than in *v100*. This difference is exacerbated by overexpressing *v100* in *n-syb* mutant neurons, leading to yet more endosomal cargo colocalization, while further ameliorating the degeneration. The genetic and cell biological interactions indicate that *n-syb* and *v100* function in concert in a neuronal sort-and-degrade mechanism (Fig. 10). The inverse correlation between endosomal accumulations and neuronal degeneration further suggests that the endosomal accumulations are not per se neurotoxic and less toxic than accumulations in late degradative compartments.

What then kills *n-syb* mutant neurons? Two main mechanisms are thought to underlie cell death in most neurodegenerative conditions. First, the neuron may become metabolically compromised when amino acids and other molecules are not recycled and accumulate in undegraded compartments; second, the accumulations themselves may be toxic. The latter hypothesis is typically discussed for accumulations in late degradative compartments, as they have a highly toxic content in terms of pH and proteases (leaky lysosomes). This idea is consistent with our observation of reduced toxicity through increased accumulations in early endosomal compartments in *n-syb* and further with *v100* overexpression in the *n-syb* mutant. We therefore speculate that the appearance of more neurotoxic late degradative compartments is the likely cause of death in *n-syb* mutant photoreceptors.

Notably, both V100 and n-Syb are synaptic proteins that have first been characterized as components of synaptic vesicles. Our finding that both proteins additionally function in neuronal maintenance through an endolysosomal sort-and-degrade mechanism suggests that the synaptic vesicle cycle may be interlinked with *v100*- and *n-syb*–mediated endosomal trafficking. Furthermore, these observations suggest the resulting maintenance function predominantly operates at synapses. We therefore propose that *v100* and *n-syb* mutants reveal a neuron-specific synaptic extension of the endolysosomal system that serves the specialized and extensive demands of neurons, and of synapses in particular, on intracellular membrane trafficking.

Materials and methods

Genetics and fly culture

Eye clones were generated using the *ey3.5FLP* system (Chotard et al., 2005; Mehta et al., 2005) to generate photoreceptor clones in otherwise heterozygous animals. The alleles *n-syb*$^{\Delta F33B}$ (Deitcher et al., 1998), *v100*^{4} (Hiesinger et al., 2005), and *syt*^{AD4} (DiAntonio et al., 1993) were used for all experiments. The transgenes upstream activation sequence (UAS)-*v100*^{WT} (Hiesinger et al., 2005), UAS-*v100*^{R755A} (Williamson et al., 2010a), UAS–*n-syb* (Bhattacharya et al., 2002), UAS-*atg1* (Scott et al., 2007), UAS-GFP-mCherry-*atg8a* (Filimonenko et al., 2007), UAS-YFP-*rab5*, UAS-YFP-*rab7*, and UAS-YFP-*rab11* (Zhang et al., 2007) have all been previously described.

For degeneration assays, flies were raised at 22°C. Flies were either exposed to standard room light for ∼12 h followed by darkness for 12 h, or they were constantly exposed to light stimulation by four light-emitting diode bulbs (2026LED-65K; 1.5 W, 30 mA) in a 30 × 30 × 40–cm aluminum foil–lined box.

Genotypes. For the analysis of mutant photoreceptors the following were used: control (ey3.5FLP;;FRT82B/FRT82B), *v100* (ey3.5FLP;;FRT82,w+,cl/FRT82Bv100^{4};Hiesingeretal.,2005),*n-syb*(ey3.5FLP;;FRT80B,w+,cl/FRT80B *n-syb*$^{\Delta F33B}$; Deitcher et al., 1998); *n-syb* rescue (ey3.5FLP;GMR-Gal4/UAS-n-syb;FRT80B,w+,cl/FRT80B *n-syb*$^{\Delta F33B}$), *syt* (ey3.5FLP;FRT40A,w+,cl/FRT40A *syt*^{AD4}; Littleton et al., 1993) TNT_inactive (GMR-Gal4>UAS-TNT-V; Sweeney et al., 1995), TNT active (GMR-Gal4>UAS-TNT-H; Sweeney et al., 1995); *atg1* expression (GMR-Gal4>UAS-atg1; Scott et al., 2007); *atg1* expression in *n-syb* photoreceptors (ey3.5FLP;GMR-Gal4/UAS-*atg1*; FRT80B,w+,cl/FRT80B *n-syb*$^{\Delta F33B}$), *tau* expression (GMR-Gal4>UAS-*tau*; Wittmann et al., 2001), *tau* expression in *n-syb* photoreceptors_(ey3.5FLP;GMR-Gal4/UAS-*atg1*; FRT80B,w+,cl/FRT80B *n-syb*$^{\Delta F33B}$), *v100* expression in *n-syb* photoreceptors (ey3.5FLP;GMR-Gal4/UAS-*v100*; FRT80B,w+,cl/FRT80B *n-syb*$^{\Delta F33B}$), and *v100-R755A* expression in *n-syb* photoreceptors (ey3.5FLP;GMR-Gal4/UAS-*v100*^{R755A}; FRT80B,w+,cl/FRT80B *n-syb*$^{\Delta F33B}$). All genotypes were verified by unequivocal markers on balancer chromosomes (Cy for CyO; Hu and Tb for TM6b, Hu, Tb; Sb for TM3, Sb) as well as independent markers (e.g., eye mosaicism, eye roughness, and antibody staining).

Immunohistochemistry, microscopy, and image processing

Adult brains and eyes, as well as pupal brains and eye–brain complexes, were dissected as previously reported (Williamson and Hiesinger, 2010b). In brief, the tissues were fixed in PBS with 3.7% formaldehyde for 30 min and washed in PBS with 0.4% Triton X-100. High-resolution light microscopy was performed at room temperature using a resonance-scanning confocal microscope (SP5; Leica) using a 63× HCX Plan Apochromat, NA 1.45, glycerin lens. Imaging data were processed and quantified using Amira 5.2 (Indeed), Photoshop (CS2; Adobe), and ImageJ (National Institutes of Health). All confocal data were obtained as 3D dataset, and all images shown are either single sections or maximum intensity projections of small subsets that were equally processed for controls and mutants. Blind deconvolution was applied as previously published (Hiesinger et al., 2001). For the quantification of up/down-regulation in mutant versus wild-type photoreceptor terminals, 50% mutant photoreceptor mosaics were created and verified using anti–n-Syb immunolabeling or other established markers. 3D confocal stacks of three to five specimens were quantified for the ratio of total fluorescence in 3 μm^3 of mutant terminals divided by total fluorescence in 3 μm^3 of wild-type terminals for each of the 16 markers individually. For the wild-type colocalization experiments, anti–n-Syb immunolabeling was analyzed for at least three specimens per colocalization experiment. For each colabeling experiment, clear and distinct n-Syb–positive punctae were selected blindly with no other channel visible. Each n-Syb–positive puncta was subsequently manually analyzed for colocalization with each of the 16 markers individually. The following antibodies were used: Syx7/Avalanche (at 1:1,000), Hrs (at 1:300), Rab5 (at 1:1,000), Rab7 (at 1:1,000), Hook (at 1:1,000), Syt (at 1:1,000), CSP (at 1:50), Chaoptin (at 1:50), V100 (at 1:2,000), and n-Syb (at 1:1,000). All confocal microscopy samples were mounted in mounting medium (Vectashield; Vector Laboratories) for fluorescence microscopy. Secondary antibodies used were Cy3, Cy5 (Jackson ImmunoResearch Laboratories, Inc.), and Alexa Fluor 488 (Invitrogen) raised against guinea pig, mouse, rabbit, or rat.

ERGs

ERGs were recorded as previously described (Fabian-Fine et al., 2003; Williamson et al., 2010a). In brief, flies were reversibly glued on slides using nontoxic school glue. Light stimulus was provided in 1-s pulses by a computer-controlled white light-emitting diode system (MC1500; Schott). Data were recorded using Clampex (version 10.1; Axon Instruments) and measured using Clampfit (version 10.2; Axon Instruments).

Western blots of mutant eye–lamina complexes, coimmunoprecipitations, and pull-downs

Eyes were dissected from 1-d-old flies in HL3 medium (Stewart et al., 1994). Groups of 20 eyes were collected in HL3 and then crushed in 10 µl extraction buffer (20 mM Tris, pH 7.4, 150 mM NaCl, 1 mM PMSF, and protease inhibitor [Complete; Roche]). Samples were incubated on ice for 15 min and then centrifuged at 16,000 RCF for 10 min at 4°C to precipitate debris. Next, 9 µl of sample was then added to 9 µl of 2× Laemmli buffer to make a final concentration of 1 eye/µl. 10 eyes were run on each lane of a 12.5% PAGE gel.

Coimmunoprecipitations. Flies were frozen in liquid nitrogen, and heads were collected with a sieve. Total protein was extracted in immunoprecipitation buffer containing 20 mM Tris, 150 mM NaCl, 1 mM PMSF, and Complete protease inhibitors, pH 7.4. The fly head extract was mixed well in 1% Triton X-100 (Bio-Rad Laboratories) and incubated for 1 h at 4°C. Samples were centrifuged at 16,000 *g* for 15 min at 4°C to remove cell debris. The resulting supernatant was incubated with 20 µl anti-Syx7 antibody (a gift from H. Krämer, University of Texas Southwestern Medical Center, Dallas, TX), 8C3 anti-Syntaxin antibody (Hiesinger et al., 2005), and anti-Syb antibody (Wu et al., 1999) coupled to protein A/G beads (Santa Cruz Biotechnology, Inc.) for 1 h at 4°C. After removing the supernatant, the beads were washed four times with immunoprecipitation buffer. A nonspecific preimmune serum was used as a control. The immunoprecipitates were eluted by boiling the beads in 50 µl SDS sample buffer and analyzed by Western blot with anti-Syb and anti-Syx7 antibodies.

GST pull-down assays. For in vivo GST pull-down assays, the GST Syx7 fusion protein was bound to glutathione–Sepharose 4B (GE Healthcare) and washed twice with standard buffer (20 mM Tris/100 mM NaCl, pH 7.4). The binding assay was performed with fly head lysis in binding buffer (20 mM Tris/150 mM NaCl, 1 mM PMSF, and Complete protease inhibitors, pH 7.4/1% Triton X-100) incubated at 4°C overnight. For in vitro GST pull-down assays, His-tagged n-Syb protein was incubated with the indicated GST fusion proteins in binding buffer (20 mM Tris/150 mM NaCl, pH 7.4/0.2% Triton X-100) at 4°C overnight. After binding, the beads were washed three times in binding buffer, and protein samples were eluted with SDS sample buffer for Western blot with anti-Syb and anti-V100 antibodies (Hiesinger et al., 2005).

EM

Newly hatched adults or staged pupae were prepared for EM and fixed as previously described (Meinertzhagen, 1996). In brief, for pupae, head capsules were carefully opened under Karnovsky fixative, and brains were dissected and split with forceps within 2 min. Tangential sections of the lamina were cut at 65 nm. Fixation was performed in modified Karnovsky fixative (Meinertzhagen, 1996) followed by veronal-buffered 2% osmium tetroxide, all as previously reported. Given that tetrad synapses are distributed relatively evenly along the length of the terminal, we sampled synaptic organelles from different levels in a single section to obtain averages. Each terminal's profile was captured with a camera (MegaView II; Kodak) and software (Soft Imaging Solutions; Olympus) at a magnification of 4,900–9,700× using a microscope (201C or Tecnai; Philips) operated at 80 kV. Samples of ≥15 terminal profiles per fly were evaluated from at least three flies per genotype. Tests of statistical significance were made between terminals from paired genotypes using a two-tailed *t* test of the means of the mean counts or measurements.

Online supplemental material

Fig. S1 shows loss of neurotransmitter release in *Drosophila* photoreceptors in a mutant for histamine synthesis does not cause degeneration. Fig. S2 shows that lack of *syb* but not *syt* in photoreceptors disrupts lamina development. Fig. S3 shows developmental analysis of synaptic terminals in the lamina. Fig. S4 shows that n-Syb does not directly interact with the early endosomal Syntaxin Syx7 and loss of *n-syb* causes more severe pro-Cathepsin accumulations than lysosomal degradation mutants. Fig. S5 shows that *n-syb* mutant synaptic terminals contain many late autophagosomal compartments. Online supplemental material is available at http://www.jcb.org/cgi/content/full/jcb.201108088/DC1.

We would like to thank Helmut Krämer, Hugo Bellen, Matt Scott, Craig Montell, Mel Feany, Stuart Newfeld, the Bloomington Stock Center, and the University of Iowa Developmental Studies Hybridoma Bank for reagents. We further thank Helmut Krämer, Jennifer Jin, Ossama Saladin, and all members of the Hiesinger laboratory for discussion and critical comments on this manuscript.

This work was supported by grants from the National Institutes of Health (RO1EY018884), the Welch Foundation (I-1657), and the Cancer Prevention Research Institute of Texas (RP100516) to P.R. Hiesinger and the National Institutes of Health (RO1EY03592) to I.A. Meinertzhagen. P.R. Hiesinger is a Eugene McDermott Scholar in Biomedical Research.

Submitted: 15 August 2011
Accepted: 20 December 2011

References

Akbar, M.A., S. Ray, and H. Krämer. 2009. The SM protein Car/Vps33A regulates SNARE-mediated trafficking to lysosomes and lysosome-related organelles. *Mol. Biol. Cell*. 20:1705–1714. http://dx.doi.org/10.1091/mbc.E08-03-0282

Antonin, W., C. Holroyd, D. Fasshauer, S. Pabst, G.F. Von Mollard, and R. Jahn. 2000. A SNARE complex mediating fusion of late endosomes defines conserved properties of SNARE structure and function. *EMBO J.* 19:6453–6464. http://dx.doi.org/10.1093/emboj/19.23.6453

Berry, D.L., and E.H. Baehrecke. 2007. Growth arrest and autophagy are required for salivary gland cell degradation in *Drosophila*. *Cell*. 131:1137–1148. http://dx.doi.org/10.1016/j.cell.2007.10.048

Bhattacharya, S., B.A. Stewart, B.A. Niemeyer, R.W. Burgess, B.D. McCabe, P. Lin, G. Boulianne, C.J. O'Kane, and T.L. Schwarz. 2002. Members of the synaptobrevin/vesicle-associated membrane protein (VAMP) family in *Drosophila* are functionally interchangeable in vivo for neurotransmitter release and cell viability. *Proc. Natl. Acad. Sci. USA*. 99:13867–13872. http://dx.doi.org/10.1073/pnas.202335999

Broadie, K., A. Prokop, H.J. Bellen, C.J. O'Kane, K.L. Schulze, and S.T. Sweeney. 1995. Syntaxin and synaptobrevin function downstream of vesicle docking in *Drosophila*. *Neuron*. 15:663–673. http://dx.doi.org/10.1016/0896-6273(95)90154-X

Burg, M.G., P.V. Sarthy, G. Koliantz, and W.L. Pak. 1993. Genetic and molecular identification of a *Drosophila* histidine decarboxylase gene required in photoreceptor transmitter synthesis. *EMBO J.* 12:911–919.

Chan, C.C., S. Scoggin, D. Wang, S. Cherry, T. Dembo, B. Greenberg, E.J. Jin, C. Kuey, A. Lopez, S.Q. Mehta, et al. 2011. Systematic discovery of Rab GTPases with synaptic functions in *Drosophila*. *Curr. Biol.* 21:1704–1715. http://dx.doi.org/10.1016/j.cub.2011.08.058

Chotard, C., W. Leung, and I. Salecker. 2005. glial cells missing and gcm2 cell autonomously regulate both glial and neuronal development in the visual system of *Drosophila*. *Neuron*. 48:237–251. http://dx.doi.org/10.1016/j.neuron.2005.09.019

Deitcher, D.L., A. Ueda, B.A. Stewart, R.W. Burgess, Y. Kidokoro, and T.L. Schwarz. 1998. Distinct requirements for evoked and spontaneous release of neurotransmitter are revealed by mutations in the *Drosophila* gene neuronal-synaptobrevin. *J. Neurosci.* 18:2028–2039.

Dermaut, B., K.K. Norga, A. Kania, P. Verstreken, H. Pan, Y. Zhou, P. Callaerts, and H.J. Bellen. 2005. Aberrant lysosomal carbohydrate storage accompanies endocytic defects and neurodegeneration in *Drosophila benchwarmer*. *J. Cell Biol.* 170:127–139. http://dx.doi.org/10.1083/jcb.200412001

DiAntonio, A., K.D. Parfitt, and T.L. Schwarz. 1993. Synaptic transmission persists in synaptotagmin mutants of *Drosophila. Cell*. 73:1281–1290. http://dx.doi.org/10.1016/0092-8674(93)90356-U

Fabian-Fine, R., P. Verstreken, P.R. Hiesinger, J.A. Horne, R. Kostyleva, Y. Zhou, H.J. Bellen, and I.A. Meinertzhagen. 2003. Endophilin promotes a late step in endocytosis at glial invaginations in *Drosophila* photoreceptor terminals. *J. Neurosci.* 23:10732–10744.

Filimonenko, M., S. Stuffers, C. Raiborg, A. Yamamoto, L. Malerød, E.M. Fisher, A. Isaacs, A. Brech, H. Stenmark, and A. Simonsen. 2007. Functional multivesicular bodies are required for autophagic clearance of protein aggregates associated with neurodegenerative disease. *J. Cell Biol.* 179:485–500. http://dx.doi.org/10.1083/jcb.200702115

Galli, T., E.P. Garcia, O. Mundigl, T.J. Chilcote, and P. De Camilli. 1995. v- and t-SNAREs in neuronal exocytosis: a need for additional components to define sites of release. *Neuropharmacology*. 34:1351–1360. http://dx.doi.org/10.1016/0028-3908(95)00113-K

Hara, T., K. Nakamura, M. Matsui, A. Yamamoto, Y. Nakahara, R. Suzuki-Migishima, M. Yokoyama, K. Mishima, I. Saito, H. Okano, and N. Mizushima. 2006. Suppression of basal autophagy in neural cells causes neurodegenerative disease in mice. *Nature*. 441:885–889. http://dx.doi.org/10.1038/nature04724

Harris, W.A., W.S. Stark, and J.A. Walker. 1976. Genetic dissection of the photoreceptor system in the compound eye of *Drosophila* melanogaster. *J. Physiol.* 256:415–439.

Heisenberg, M. 1971. Separation of receptor and lamina potentials in the electroretinogram of normal and mutant *Drosophila*. *J. Exp. Biol.* 55:85–100.

Hiesinger, P.R., C. Reiter, H. Schau, and K.F. Fischbach. 1999. Neuropil pattern formation and regulation of cell adhesion molecules in *Drosophila* optic lobe development depend on synaptobrevin. *J. Neurosci.* 19:7548–7556.

Hiesinger, P.R., M. Scholz, I.A. Meinertzhagen, K.F. Fischbach, and K. Obermayer. 2001. Visualization of synaptic markers in the optic neuropils of *Drosophila* using a new constrained deconvolution method. *J. Comp. Neurol.* 429:277–288. http://dx.doi.org/10.1002/1096-9861(20000108)429:2<277::AID-CNE8>3.0.CO;2-8

Hiesinger, P.R., A. Fayyazuddin, S.Q. Mehta, T. Rosenmund, K.L. Schulze, R.G. Zhai, P. Verstreken, Y. Cao, Y. Zhou, J. Kunz, and H.J. Bellen. 2005. The v-ATPase V0 subunit a1 is required for a late step in synaptic vesicle exocytosis in *Drosophila. Cell*. 121:607–620. http://dx.doi.org/10.1016/j.cell.2005.03.012

Hiesinger, P.R., R.G. Zhai, Y. Zhou, T.W. Koh, S.Q. Mehta, K.L. Schulze, Y. Cao, P. Verstreken, T.R. Clandinin, K.F. Fischbach, et al. 2006. Activity-independent prespecification of synaptic partners in the visual map of *Drosophila. Curr. Biol.* 16:1835–1843. http://dx.doi.org/10.1016/j.cub.2006.07.047

Komatsu, M., S. Waguri, T. Chiba, S. Murata, J. Iwata, I. Tanida, T. Ueno, M. Koike, Y. Uchiyama, E. Kominami, and K. Tanaka. 2006. Loss of autophagy in the central nervous system causes neurodegeneration in mice. *Nature*. 441:880–884. http://dx.doi.org/10.1038/nature04723

Krantz, D.E., and S.L. Zipursky. 1990. *Drosophila* chaoptin, a member of the leucine-rich repeat family, is a photoreceptor cell-specific adhesion molecule. *EMBO J.* 9:1969–1977.

Lee, J.H., W.H. Yu, A. Kumar, S. Lee, P.S. Mohan, C.M. Peterhoff, D.M. Wolfe, M. Martinez-Vicente, A.C. Massey, G. Sovak, et al. 2010. Lysosomal proteolysis and autophagy require presenilin 1 and are disrupted by Alzheimer-related PS1 mutations. *Cell*. 141:1146–1158. http://dx.doi.org/10.1016/j.cell.2010.05.008

Lee, S.J., and C. Montell. 2004. Suppression of constant-light-induced blindness but not retinal degeneration by inhibition of the rhodopsin degradation pathway. *Curr. Biol.* 14:2076–2085. http://dx.doi.org/10.1016/j.cub.2004.11.054

Littleton, J.T., M. Stern, K. Schulze, M. Perin, and H.J. Bellen. 1993. Mutational analysis of *Drosophila* synaptotagmin demonstrates its essential role in Ca(2+)-activated neurotransmitter release. *Cell*. 74:1125–1134. http://dx.doi.org/10.1016/0092-8674(93)90733-7

Lu, H., and D. Bilder. 2005. Endocytic control of epithelial polarity and proliferation in *Drosophila*. *Nat. Cell Biol.* 7:1232–1239. http://dx.doi.org/10.1038/ncb1324

McPhee, C.K., and E.H. Baehrecke. 2009. Autophagy in *Drosophila melanogaster*. *Biochim. Biophys. Acta*. 1793:1452–1460. http://dx.doi.org/10.1016/j.bbamcr.2009.02.009

Mehta, S.Q., P.R. Hiesinger, S. Beronja, R.G. Zhai, K.L. Schulze, P. Verstreken, Y. Cao, Y. Zhou, U. Tepass, M.C. Crair, and H.J. Bellen. 2005. Mutations in *Drosophila* sec15 reveal a function in neuronal targeting for a subset of exocyst components. *Neuron*. 46:219–232. http://dx.doi.org/10.1016/j.neuron.2005.02.029

Meinertzhagen, I.A. 1996. Ultrastructure and quantification of synapses in the insect nervous system. *J. Neurosci. Methods*. 69:59–73. http://dx.doi.org/10.1016/S0165-0270(96)00021-0

Nixon, R.A., D.S. Yang, and J.H. Lee. 2008. Neurodegenerative lysosomal disorders: a continuum from development to late age. *Autophagy*. 4:590–599.

Reist, N.E., J. Buchanan, J. Li, A. DiAntonio, E.M. Buxton, and T.L. Schwarz. 1998. Morphologically docked synaptic vesicles are reduced in synaptotagmin mutants of *Drosophila. J. Neurosci.* 18:7662–7673.

Schoch, S., F. Deák, A. Königstorfer, M. Mozhayeva, Y. Sara, T.C. Südhof, and E.T. Kavalali. 2001. SNARE function analyzed in synaptobrevin/VAMP knockout mice. *Science*. 294:1117–1122. http://dx.doi.org/10.1126/science.1064335

Schultz, M.L., L. Tecedor, M. Chang, and B.L. Davidson. 2011. Clarifying lysosomal storage diseases. *Trends Neurosci.* 34:401–410. http://dx.doi.org/10.1016/j.tins.2011.05.006

Scott, R.C., G. Juhász, and T.P. Neufeld. 2007. Direct induction of autophagy by Atg1 inhibits cell growth and induces apoptotic cell death. *Curr. Biol.* 17:1–11. http://dx.doi.org/10.1016/j.cub.2006.10.053

Stewart, B.A., H.L. Atwood, J.J. Renger, J. Wang, and C.F. Wu. 1994. Improved stability of *Drosophila* larval neuromuscular preparations in haemolymph-like physiological solutions. *J. Comp. Physiol. A Neuroethol. Sens. Neural Behav. Physiol.* 175:179–191. http://dx.doi.org/10.1007/BF00215114

Südhof, T.C., and J.E. Rothman. 2009. Membrane fusion: grappling with SNARE and SM proteins. *Science*. 323:474–477. http://dx.doi.org/10.1126/science.1161748

Sweeney, S.T., and G.W. Davis. 2002. Unrestricted synaptic growth in spinster-a late endosomal protein implicated in TGF-beta-mediated synaptic growth regulation. *Neuron*. 36:403–416. http://dx.doi.org/10.1016/S0896-6273(02)01014-0

Sweeney, S.T., K. Broadie, J. Keane, H. Niemann, and C.J. O'Kane. 1995. Targeted expression of tetanus toxin light chain in *Drosophila* specifically eliminates synaptic transmission and causes behavioral defects. *Neuron*. 14:341–351. http://dx.doi.org/10.1016/0896-6273(95)90290-2

Tooze, S.A., and G. Schiavo. 2008. Liaisons dangereuses: autophagy, neuronal survival and neurodegeneration. *Curr. Opin. Neurobiol.* 18:504–515. http://dx.doi.org/10.1016/j.conb.2008.09.015

Uytterhoeven, V., S. Kuenen, J. Kasprowicz, K. Miskiewicz, and P. Verstreken. 2011. Loss of skywalker reveals synaptic endosomes as sorting stations for synaptic vesicle proteins. *Cell*. 145:117–132. http://dx.doi.org/10.1016/j.cell.2011.02.039

Williamson, W.R., and P.R. Hiesinger. 2010a. On the role of v-ATPase V0a1-dependent degradation in Alzheimer disease. *Commun Integr Biol*. 3:604–607. http://dx.doi.org/10.4161/cib.3.6.13364

Williamson, W.R., and P.R. Hiesinger. 2010b. Preparation of developing and adult *Drosophila* brains and retinae for live imaging. *J. Vis. Exp.* 37:1936. http://dx.doi.org/10.3791/1936

Williamson, W.R., D. Wang, A.S. Haberman, and P.R. Hiesinger. 2010a. A dual function of V0-ATPase a1 provides an endolysosomal degradation mechanism in *Drosophila melanogaster* photoreceptors. *J. Cell Biol.* 189:885–899. http://dx.doi.org/10.1083/jcb.201003062

Williamson, W.R., T. Yang, J.R. Terman, and P.R. Hiesinger. 2010b. Guidance receptor degradation is required for neuronal connectivity in the *Drosophila* nervous system. *PLoS Biol.* 8:e1000553. http://dx.doi.org/10.1371/journal.pbio.1000553

Wittmann, C.W., M.F. Wszolek, J.M. Shulman, P.M. Salvaterra, J. Lewis, M. Hutton, and M.B. Feany. 2001. Tauopathy in *Drosophila*: neurodegeneration without neurofibrillary tangles. *Science*. 293:711–714. http://dx.doi.org/10.1126/science.1062382

Wu, M.N., T. Fergestad, T.E. Lloyd, Y. He, K. Broadie, and H.J. Bellen. 1999. Syntaxin 1A interacts with multiple exocytic proteins to regulate neurotransmitter release in vivo. *Neuron*. 23:593–605. http://dx.doi.org/10.1016/S0896-6273(00)80811-9

Xu, H., S.J. Lee, E. Suzuki, K.D. Dugan, A. Stoddard, H.S. Li, L.A. Chodosh, and C. Montell. 2004. A lysosomal tetraspanin associated with retinal degeneration identified via a genome-wide screen. *EMBO J.* 23:811–822. http://dx.doi.org/10.1038/sj.emboj.7600112

Zhang, J., K.L. Schulze, P.R. Hiesinger, K. Suyama, S. Wang, M. Fish, M. Acar, R.A. Hoskins, H.J. Bellen, and M.P. Scott. 2007. Thirty-one flavors of *Drosophila* rab proteins. *Genetics*. 176:1307–1322. http://dx.doi.org/10.1534/genetics.106.066761